NPL REPORT
CIRM 51

The NPL contribution to a CCRI international comparison of fast neutron fluence measurements performed at the PTB in March 2001

David J. Thomas, Neil J. Roberts,
Andrew Bennett, Peter Kolkowski

April 2002

April 2002

NATIONAL PHYSICAL LABORATORY

The NPL contribution to a CCRI international comparison of fast neutron fluence measurements performed at the PTB in March 2001

by

David J. Thomas, Neil J. Roberts,
Andrew Bennett, Peter Kolkowski

Centre for Ionising Radiation Metrology

Abstract

This report contains details of the experimental procedures used by NPL during an international comparison of fast neutron fluence measurements at four energies, namely, 144 keV, 1.2 MeV, 5.0 MeV and 14.8 MeV. The measurements were performed at the Physikalisch- Technische Bundesanstalt, PTB, Braunschweig. A description is also given of the analysis technique and the various corrections applied. The final results for the fluence per monitor count are given together with a detailed breakdown of the uncertainties.

ISSN 1369-6793

National Physical Laboratory
Teddington, Middlesex, United Kingdom, TW11 0LW

Approved on behalf of Managing Director, NPL, by
Dr Martyn Sené, Head, Centre for Ionising Radiation Metrology

CONTENTS

Page

1 Introduction

A number of international comparisons of monoenergetic fast neutron fluence measurements have been carried out over the years. These have been organised under the auspices of the Comité Consultatif pour les Rayonnements Ionisants, CCRI, (previously the Comité Consultatif pour les Étalons de Mesure des Rayonnements Ionisants, CCEMRI). A discussion of the comparisons completed prior to 1992 can be found in reference 1. These exercises were undertaken to compare and validate neutron metrology standards, and to improve accuracy by investigating matters such as: systematic errors, the measurement methods, the instruments used, and the corrections applied at different national laboratories.

Fast neutron fluence comparisons tend to be undertaken at the energies recommended by the International Organization for Standardization, ISO, for performing calibrations [(2)]. In the past they have been carried out by circulating a transfer device. A comparison would thus involve a measurement by each participating laboratory of the fluence response of the transfer device at a fixed neutron energy. This approach has certain advantages. It is a test of a laboratory's capability to both produce a monoenergetic fluence at a particular energy, and also to measure that fluence. There are, however, disadvantages to the use of a transfer device. Firstly, the whole process of circulating the device to several laboratories is very slow, the comparison tends to lose momentum, and the complete exercise can take many years. Secondly, the transfer device must be completely stable with time. Any uncertainties introduced by the transfer device, in particular those due to instability, are components of the final uncertainty budget, and these can mask genuine differences in standards.

In an attempt to overcome these disadvantages, in particular to speed-up the exercise, a type of comparison, novel in the area of neutron fluence metrology[*], has been undertaken where all the participants measured a selection of fast neutron fields produced at the German national standards laboratory, Physikalisch- Technische Bundesanstalt, PTB, in Braunschweig. One of the main reasons for adopting this approach and speeding up the comparison process, was the recently introduced concept of national laboratories being deemed 'equivalent' in terms of providing standards in particular areas. The equivalence is proved by participation in a *key* comparison and obtaining agreement, within the uncertainties, with a reference value derived by the comparison evaluator. In order to be valid a key comparison must have taken place during the last ten years, and no fast neutron comparison exercise has been completed in the ten years prior to 2001. (A comparison of 24 keV fluence measurements undertaken during this period is still not finalised.)

Performing the comparison at one establishment removes one important aspect of realising a neutron fluence standard, i.e. the production of the field, for all but one of the participants. Nevertheless, the exercise undertaken at PTB is important and timely, and the fact that all participants measured the same fields provides a particularly stringent test of the fluence measuring techniques.

For the present exercise four of the ISO recommended energies were chosen, namely: 144 keV, 1.2 MeV, 5.0 MeV, and 14.8 MeV. The fields were all produced by charged particle induced reactions using ion beams from the PTB 3.5 MV Van de Graaff accelerator. Each

[*] A comparison of neutron absorbed dose measurements was organised in this way in 1983, see reference 1.

participating laboratory was required to provide their best estimates of the neutron fluences in vacuum, at 0^o to the charged particle beam direction, and at 1m from the neutron producing target. It was necessary to quote the fluences relative to the reading of an appropriate monitor. A full uncertainty budget was also required for each energy.

The comparison exercise was performed over a two week period with three participants (in addition to PTB) making their measurements each week. ETL (Japan), IRMM (European Community), VNIIM (Russia), and PTB (Germany) made measurements during the first week (19^{th} - 23^{rd} March 2001), and CIAE (China), NIST (USA), NPL (UK), and PTB during the second week (26^{th} - 30^{th} March 2001).

The Van de Graaff accelerator was run for 24 hours a day, with one day assigned to each of the four energies. Measurements of the fluences were made in shifts, with PTB making measurements at the start and end of each day. Time was nominally divided equally between the participants, however this was flexible as some participant's measurements required longer or shorter allocations of time at particular energies.

Participants were expected, wherever possible, to measure the fluences using the same instrumentation as normally employed at their own laboratories.

2 Neutron fluence standardisation techniques used at NPL

2.1 The energy range from a few keV to 5 MeV

Fluence measurements for monoenergetic neutron fields produced at NPL in the range from a few keV to about 5 MeV are performed using one of two long counters. A long counter consists essentially of a BF_3 proportional counter positioned along the axis of a cylindrical moderator. By careful design of the moderator configuration the response to neutrons incident on one end of the cylinder is roughly constant as a function of energy over the range from a few keV to 5 MeV or higher.

The two long counters available at NPL are of different types. One, built in-house, is a McTaggart type [3]. This instrument, commonly called the NPL standard long counter, and designated here as 'the NPL LC', has the advantage of high efficiency, of the order of 12 cm^2, over the above energy range. (The efficiency is given as counts per [neutron per cm^2], hence the units cm^2.) However, this instrument is particularly large, being roughly 61 cm long by 46 cm diameter, and the moderator, being paraffin wax, is not particularly stable. The second long counter is of the De Pangher type [4]. This instrument, illustrated in Figure 1, is smaller, being 43 cm long with a roughly 39 cm diameter moderator. This moderator is made of polyethylene and is hence much more robust.

Because they are made to very tight tolerances, De Pangher long counters have the useful feature that the response functions of all counters of this type should have the same shape. The overall normalisation of the response function depends on the particular BF_3 tube used, but if a correction is made for the efficiency of the tube, the calibration of one De Pangher long counter can in principle be transferred to any other. Unfortunately the efficiency of the De Pangher long counter is almost a factor of four less than that of the NPL LC. Nevertheless, it is still a high-efficiency device by the standards of most neutron measuring instruments, and because of its smaller physical size and robustness was chosen for the present exercise.

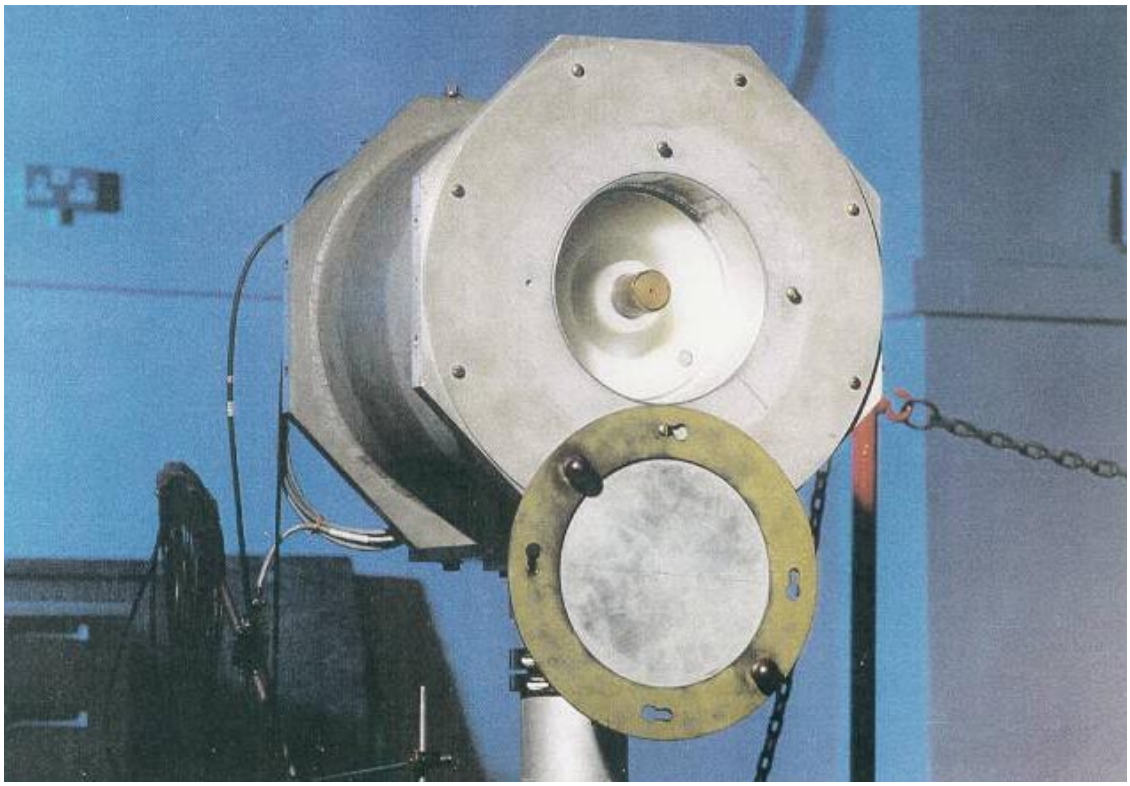

Figure 1. The De Pangher long counter, shown with cadmium cover lowered to reveal the front moderator surface and the end of the BF_3 proportional counter tube.

A long counter is not an absolute instrument and therefore needs to be calibrated. The fluence response functions of the NPL long counters were determined in the early 1970s using a number of approaches. Several different radionuclide neutron sources, with emission rates measured absolutely in the NPL manganese sulphate bath, and with a range of mean energies, were used to calibrate the long counters. These data were combined with the results of an empirical formula predicting the response in the region above 2.8 MeV to give a 'working' response function. The values obtained in this way were confirmed, relative to the hydrogen scattering cross-section, over the neutron energy range from 2.5 MeV to 5.5 MeV using a proton recoil telescope of conventional design. They were also checked absolutely over the neutron energy range from 0.5 MeV to 1 MeV using the associated target activity technique. A description of these procedures is given in NPL Report RS(EXT)5 [(5)].

When making measurements of fluence from a point source, a long counter can, provided the source to counter distance is reasonably large (≥1m), be regarded as a point detector. The position of this point, measured relative to the front moderator face of the long counter and commonly called the effective centre, must be known accurately as a function of neutron energy. A table of effective centre values, based on measurements made over a range of source to detector distances, with both radionuclide source neutrons and monoenergetic neutrons [(5)], has been in use at NPL since the mid 1970s.

Recently work has been undertaken to improve knowledge of both the efficiencies and effective centres of the long counters. Modern Monte Carlo techniques, in particular the use of the radiation transport code MCNP [(6)], offer the possibility of performing accurate calculations

of long counter response functions. A project to perform these calculations and to compare the results with both new and old measurements with radionuclide sources has recently been completed [7]. The calculated efficiency values are in good agreement with the measurements, and should provide an improved database of efficiency values for use in determining neutron fluences.

A calculation of the effective centre cannot be performed directly. A technique has, however, been devised whereby the response of the long counter is calculated at a large number of distances from a point source. By analysing these data in the same way as a set of experimental data, a value can be derived for the effective centre. These calculated effective centres exhibit sharp, and as yet unexplained, variations with energy. Agreement with experiments is not uniformly good, and the experiments themselves exhibit problems of repeatability. Work on improving effective centre values is not yet complete, and a reliable validated set of revised effective centres is not presently in place. The calculated data are available for use, however, because of the disagreement between calculation and measurement, an increased uncertainty has to be assigned to these effective centre values.

The measurements at PTB have been analysed using both the 'old' set of efficiencies and effective centres, and also the 'new' efficiency values together with the new calculated effective centres. It is hoped that the present comparison exercise will cast light on the best combination to use.

2.2 The energy range 13.5 to 14.7 MeV

Neutrons with mean energies ranging from about 13.5 to 14.7 MeV are produced at the NPL by using beams of deuterons from a 150 kV 'SAMES' accelerator to bombard a tritium target. Neutrons and alpha particles are emitted in the fusion reaction $T(d,n)^4He$ which is exothermic with a Q value of 17.59 MeV. The reaction has a resonance at about 110 keV thus enabling intense high energy neutron fields to be produced with this relatively low-energy accelerator.

There are two primary techniques for the measurement of d + T neutron fluences from an accelerator of this type. The first involves measuring the associated alpha particle, AAP, emission in a well defined solid angle[8]. The second method relies on the accurately known neutron-proton scattering cross section and involves the use of a proton recoil telescope, PRT. Routine d + T fluence measurements are performed at NPL using the AAP technique, and this approach has been compared with a PRT with excellent agreement[9]. The PRT is not used routinely, and since the detector for measuring the AAPs is an integral part of the accelerator beam line facility neither technique was applicable for the present comparison exercise.

There is a third technique used at NPL to measure d + T neutron fluences, and that is the activation in thin foils. An activation measurement is a secondary standard technique, however, the cross sections of some activation reactions are so accurately known that this approach provides results of comparable accuracy to the two absolute techniques. The technique is an excellent transfer standard for neutron measurements at laboratories other than NPL, and was hence ideal for the present comparison exercise.

Two activation reactions are used routinely at NPL, these are, $^{27}Al(n,\alpha)^{24}Na$ and $^{56}Fe(n,p)^{56}Mn$. For both of these reactions the product nucleus is a β emitter with a reasonably simple decay scheme, particularly simple in the case of ^{24}Na. Their activities can be measured

using $4\pi\beta$-γ coincidence counting, or if the foil β-counting efficiency is known, by β-counting alone. The foils used at NPL have had their β-counting efficiency measured by $4\pi\beta$-γ counting following activation in a high neutron fluence. When foil activities are low, simple β-counting is the preferred option since this allows the use of an anti-coincidence shielded low-background counter thus reducing the effects of background.

The isotope ^{56}Mn has a half-life of about 2.6 hours, and this is far too short to contemplate activation at PTB with return to NPL for counting. The chosen reaction was therefore ^{27}Al(n,α)^{24}Na, where the induced ^{24}Na has a half life of about 15 hours. This is still relatively short and special arrangements were made to return the foils to NPL as quickly as possible. The cross section for this reaction is about 112 mb at 14.8 MeV requiring a minimum fluence of the order of 5×10^9 cm^{-2} in order to make a measurement viable. (More is required if there is going to be a significant delay before foil counting can begin.)

There is a competing reaction which occurs in aluminium when irradiated with 14.8 MeV neutrons, and that is ^{27}Al(n,p)^{27}Mg. The half life of the induced ^{27}Mg is, however, only 9.46 minutes and it therefore decays away quickly.

Neutron fluences in the energy range from 13.5 to 14.7 MeV are produced at the NPL in a separate experimental area to those produced using the Van de Graaff accelerator. The long counters are situated in the experimental area associated with the Van de Graaff, and are not in general used for measuring d + T fluences. Efficiencies and effective centres are, however, available for the long counters in the 14 MeV region, albeit with higher uncertainties than at energies below 5 MeV, and it was therefore thought worthwhile to undertake measurements at PTB with the long counters at 14.8 MeV. These measurements should act as a check on the foil measurements and provide information about the De Pangher efficiency at these energies.

3 Long counter check measurements pre- and post-comparison

3.1 Comparison of measurements with the NPL LC and the De Pangher

Although fluence measurements at NPL are performed with both the NPL LC and the De Pangher, the NPL LC is more commonly used. For this reason comparisons were made, prior to the PTB measurements, of fluence determinations with the two devices. Monoenergetic fluences, of the same energies as those used in the comparison (with the exception of 14.8 MeV), were produced using beams from the NPL Van de Graaff accelerator, and the same neutron producing reactions as subsequently used in the PTB measurements.

Corrections for in-scatter were made using shadow cones, and for air out-scatter by applying an exponential attenuation coefficient. Pulses from a current integrator, which measured the charge on the neutron producing target, were used as monitor counts to relate the two long counter results. Measurements were made at a number of distances (all at 0° to the charged particle beam) and the mean values for the fluence per current integrator pulse are given in Table 1. The columns labelled “old” correspond to analysis using the old efficiency and effective centre values, while those labelled “new” give the results using the most recent efficiency and effective centre values. Fluences are quoted at 1 cm from the target which is the usual convention at NPL.

Table 1. Comparison of fluence measurements at NPL with the NPL LC and the De Pangher

Neutron energy	Mean fluence at 1 cm per current integrator pulse (cm^{-2})				Ratio (NPL/De Pangher)	
	NPL LC old	NPL LC new	De Pangher old	De Pangher new	old	new
144 keV	7.051×10^5 ± 2.1%	7.163×10^5 ± 2.1%	6.949×10^5 ± 2.1%	7.149×10^5 ± 2.1%	1.015 ± 0.030	1.002 ± 0.030
1.2 MeV	6.106×10^3 ± 2.4%	6.426×10^3 ± 2.4%	6.023×10^3 ± 2.4%	6.268×10^3 ± 2.4%	1.014 ± 0.034	1.025 ± 0.035
5.0 MeV	2.570×10^4 ± 2.2%	2.458×10^4 ± 2.2%	2.502×10^4 ± 2.2%	2.492×10^4 ± 2.2%	1.027 ± 0.032	0.986 ± 0.031
Mean ratio (NPL/De Pangher): old = 1.019 ± 0.004 new = 1.004 ± 0.011 The uncertainties shown for the mean ratios in the two lines above are the standard errors of the means derived from the spread of the ratio values.						

The uncertainties quoted for the mean fluences are derived from the uncertainties of the measurements at each distance. These in turn have come from combining the statistical, dead-time, scatter corrections, effective distance, and efficiency uncertainty components. Some of the uncertainty components, e.g. the long counter efficiency, are common to measurements at different distances. Some, such as the statistical uncertainty, are completely uncorrelated. Some, such as the uncertainty introduced by the air out-scatter correction and the uncertainty in the effective centre value, are partially correlated. This complicates the uncertainty analysis, and this issue is discussed in Section 7 in relation to the measurements at the PTB. The uncertainties quoted in Table 1 represent reasonable estimates of the combined uncertainty in the fluence as obtained from a small number of readings at different distances. Uncertainties in the ratios come from the propagation of the uncertainties in the two components. The uncertainties for the mean ratios come from the spread of the results and are smaller than would be expected from the uncertainties in the individual ratios.

Table 1 provides good evidence that, within the estimated uncertainties, the two long counters give the same results for the measured fluence, provided the same 'vintage' parameters are used, i.e. either the old or the new, for both long counters. For the old values of the parameters there is some suggestion of a bias with the NPL LC values being higher than those measured with the De Pangher, but this is not significant within the uncertainties.

3.2 Stability of the De Pangher long counter

Approximately four times a year the response of the NPL De Pangher long counter is checked using a small ^{241}Am-Be(α,n) neutron source which is inserted in an accurately reproducible way into a hole in the polythene moderator. Some additional checks were performed immediately before and after the PTB comparison exercise. Figure 2 shows how the measured count rate for the source (corrected for decay) varied over time.

From the figure it is obvious that the variations in the counts were considerably larger than expected from statistics – indicated by the error bars which show the statistical standard uncertainty on the measurements. No explanation for these variations is available at present.

Certainly variations in the cosmic ray background are far too small as evidenced by repeat measurements of the background over many years. One possible cause is variation of the effective discriminator level in the electronics. Regardless of the cause, however, the variations are very small, the standard deviation on a number of readings being of the order of 0.4% indicating very good long term stability.

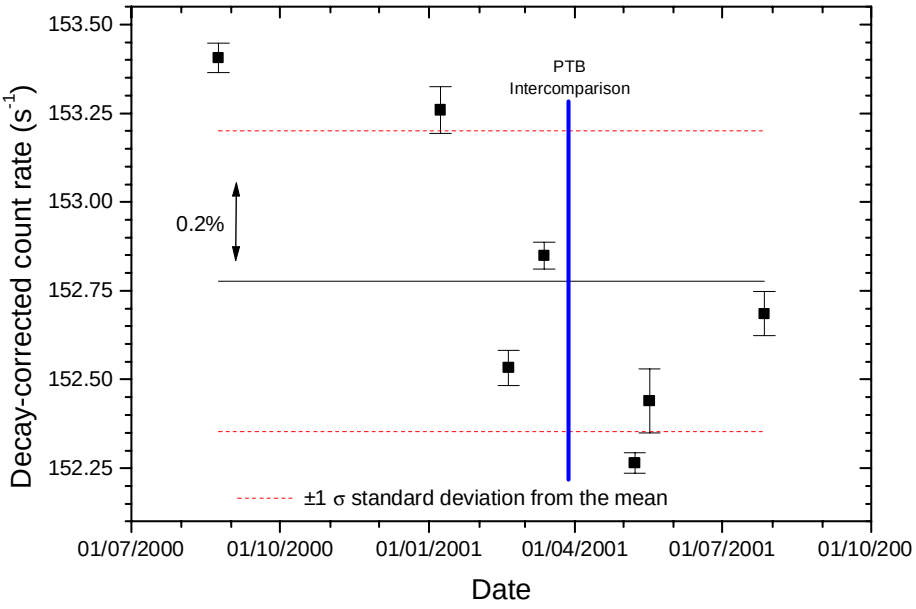

Figure 2. De Pangher check source measurements before and after the PTB comparison

4 Measurements at the PTB

4.1 Neutron field production

The four energies used in the comparison exercise were all produced by different reactions. Table 2 gives details, provided by the PTB [10], of these reactions, and also of the charged particle beam energies, the target characteristics, and the mean energy loss for the particle beam traversing the target material. This last number gives a good idea of the energy width of the primary neutron distribution since the energy width of the charged particle beam (FWHM 2 to 4 keV) is considerably smaller.

Table 2. Details of the neutron field production at PTB

Neutron energy	Reaction	Charged particle beam energy (MeV)	Target material	Target characteristics	Charged particle energy loss in target
144 keV	$^{7}Li(p,n)^{7}Be$	1.947	LiOH	36 µg cm^{-2} layer	21 keV
1.2 MeV	$^{3}H(p,n)^{3}He$	2.050	Tritium absorbed in titanium	937 µg cm^{-2} titanium layer	97 keV
5.0 MeV	$^{2}H(d,n)^{3}He$	2.300	Deuterium gas	710 hPa of gas	137 keV

14.8 MeV	$^{3}H(d,n)^{4}He$	0.242	Tritium absorbed in titanium	1080 μg cm^{-2} titanium layer	229 keV

4.2 Measurements with the NPL De Pangher long counter

All the measurements were performed in the experimental hall of the Chadwick Bau, PTB. This is shown schematically in Figure 3. The De Pangher long counter was mounted on a lightweight support fixed to a trolley on the fourth swivel arm clockwise from the beam line (labelled arm 6). Theodolites mounted at fixed positions were used to align the height and direction of the long counter. All fluence measurements were made at 0° to the charged particle beam from the accelerator, but it was necessary to move the long counter after the fluence had been measured at each energy to allow the other participants to make their measurements. The position and alignment of the long counter therefore had to be checked for each energy.

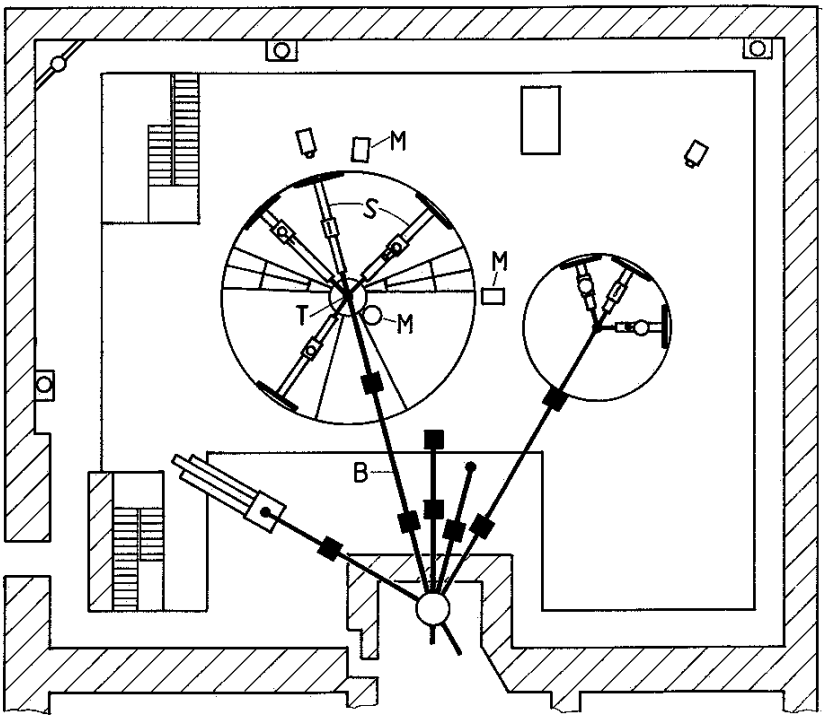

Figure 3. PTB experimental hall, 30 m wide, 24 m deep and 14 m high, used for calibrations with monoenergetic neutrons. (B = beam line; T = neutron producing target; S = four swivel arms with movable detector supports; M = neutron and photon monitors)

In-scatter measurements were made using two shadow cones from the NPL set (numbers 1 and 8). These are both 50 cm long with the first 20 cm of each one being iron and the second 30 cm borated paraffin wax. Cone 1 has a diameter of 3.2 cm at the narrow end and an angle of 5.03°. The corresponding values for cone 8 are 3.5 cm and 9.70°. At 1.2 MeV additional measurements were made using two PTB shadow cones (numbers 15 and 19). The cones were mounted on a movable trolley located on the small circle at the centre of the pit. A different, and significantly more massive, base plate was used to mount the NPL shadow cones on the support stand than was used for the PTB shadow cones. Theodolites were again used to check the correct height, position and alignment of the cones.

Measurements of the fluence at each energy were made with the long counter at several different distances from the target. The number of distances ranged from 3 to 6, depending on the count rate and the time available, and were all in the range 150 cm to 400 cm. The distance from the target to the front of the polythene moderator of the long counter (with the cadmium cover removed) was measured each time. For in-scatter measurements at each distance, the appropriate shadow cone was used (number 1 for distances greater than 250 cm, and number 8 for distances less than or equal to 250 cm), with the narrow end of the cone at the distance from the target normally used at NPL.

Neutrons at 5 MeV were produced using a deuterium gas target. Some neutrons are produced from D(d,n) reactions in deuterons implanted in the gold layer at the back of the target. To deduct these neutrons from the total fluence measurement it was necessary to make a 'gas-out' measurement where the deuterium gas was removed from the target. A 'gas-out' measurement was performed at each long counter distance, and as a result, the target had to be refilled for each new distance. It was not possible to refill the target to the exact same gas pressure each time, and so the number of deuterium nuclei in the target was not the same for measurements at all distances, this has implications for the monitor used.

The signal from the pre-amplifier, positioned on the back of the De Pangher long counter was fed through to the experimental control room where it was connected to a conventional pulse counting electronic chain consisting of a main amplifier and single channel analyser, SCA. The signal from the SCA was fed into a width/delay unit, which imposed a fixed dead-time, and the output from the width/delay was counted in a scaler system. All units were brought from NPL. The SCA discriminator level was set and monitored throughout the measurements by viewing the gated and ungated pulse height spectra on a portable MCA system (see Figure 4), also brought from NPL. In addition to recording the counts in the long counter, the scalers also logged counts from the monitors provided by the PTB.

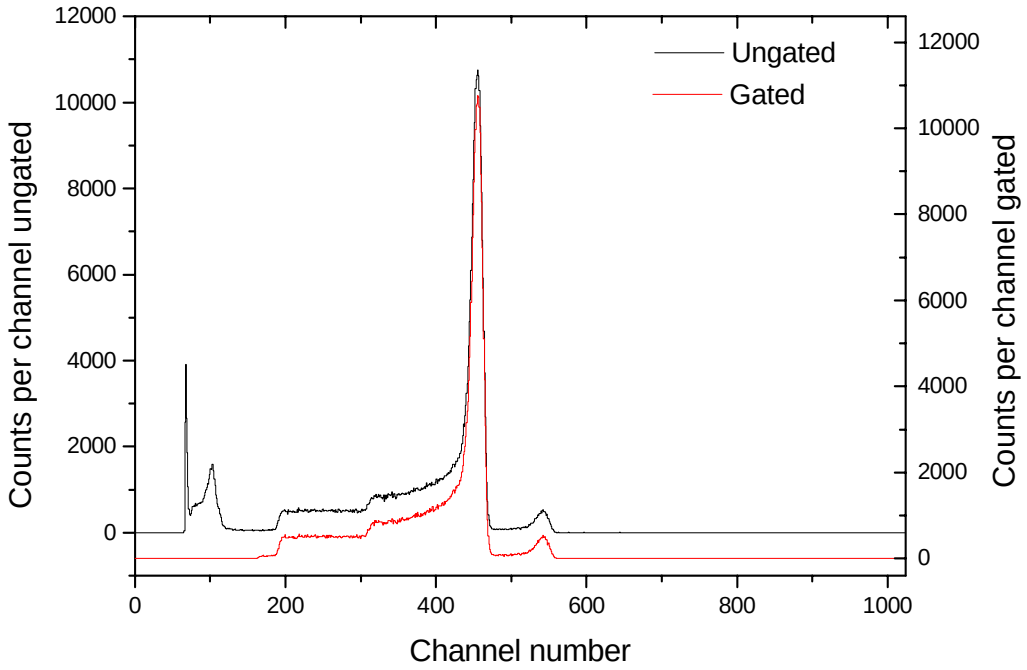

Figure 4. Ungated and gated pulse height spectra from the BF_3 tube

The measurement at each distance was divided into a number of consecutive cycles having a fixed number of pulses from a current integrator measuring the beam charge. This approach enabled the stability of the long counter and the monitors to be checked by comparing the observed and theoretical counting uncertainties.

4.3 Foil irradiations

Measurement of the neutron fluence at 14.8 MeV was performed by irradiating two aluminium foils of thickness 0.26 mm and diameter 25 mm. The two foils were joined back-to-back using adhesive tape and held in a lightweight phosphor bronze mount fixed to the shadow cone stand at 0° to the beam line (see Figure 5). The distance of the front foil from the target face was set to be 90.0 mm. This was achieved by inserting a measuring rod between the target and the foils, then moving the mounting assembly towards the target until the front foil touched the rod. The height and alignment of the foils were checked using the theodolites.

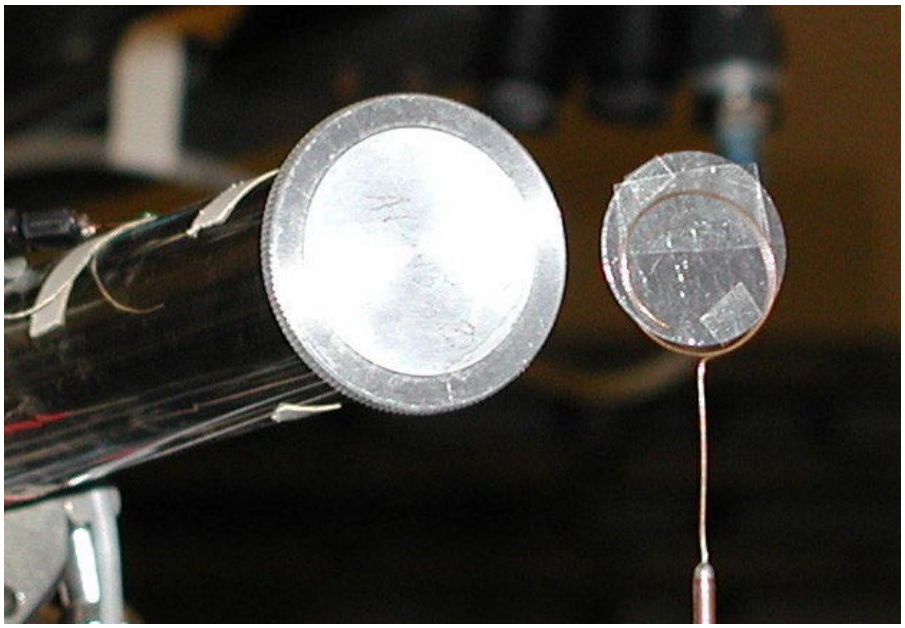

Figure 5. Mounting arrangement of the aluminium foils
at 90 mm from the end of the target can

The foils were irradiated for 12800 seconds. The start time of the irradiation was taken from the German national time signal. The time was also checked with the NPL clock signal by telephone. During the irradiation, the three monitor signals were recorded as before.

A member of staff took the foils back to NPL by plane for analysis. Foil counting began within 7 hours of the end of the irradiation.

4.4 Fluence monitoring

To normalise the different measurements made at each energy by each participant, PTB provided three methods for monitoring the fluence:

1. a current integrator, CI, provided pulses corresponding to a fixed amount of charge collected at the target, and hence to a fixed number of protons or deuterons incident on the target
2. a De Pangher precision long counter, PLC, located at 97° to the beam line and ~5m from the target gave a direct measure of the neutrons produced,
3. a second neutron monitor (referred to as the New Monitor, NM) located at ~17.5° to the beam line and ~5m from the target also gave a measure of the neutrons produced.

Figure 3 shows the locations of the two monitors, the third monitor shown in this plan, situated close to the target, is a Geiger Müller tube used for measuring the photon field.

5 Analysis

5.1 Monitor data

The three monitors made available to normalise the fluence measurements of the various participants have various advantages and disadvantages. The CI, measuring the current on the neutron producing target, provides a good measure of neutron production, provided the target characteristics, i.e. target thickness in the case of the lithium target, and gas loading in the case of the tritium and deuterium targets, remain constant. If the targets are not completely uniform over their area, there is also the requirement that the beam 'spot' profile on the target does not change.

The other two monitors, the NM and the PLC, measure neutrons directly. They suffer, however, from the fact that their readings are affected by the presence of whatever devices are present in the neutron field in the vicinity of the target. These can scatter neutrons into, or away from, the monitors. Since the quantity required for the present comparison exercise is the fluence at 1 m from the target, in the absence of the fluence measuring equipment, corrections needed to be applied to allow for the presence of the NPL De Pangher long counter, and of a shadow cone if one was present, by correcting the NM and PLC readings to what they would have been in the absence of these objects.

Monitor correction factors for the NM were provided by the PTB. These were obtained from CI and NM readings taken by the PTB staff during the measurements by the participants, and also for so-called 'free field' arrangements. For the free field measurements all fluence measuring equipment was moved as far away as possible from the neutron producing target to reduce scatter into the monitors to a negligibly low level. The ratios of the monitor readings for the two different arrangements provided the correction factors.

The measurements of the monitor corrections depend on a stable measure of the neutron output to relate the free field measurements to those with the fluence measuring equipment in place. The device used to measure the output was the current integrator. The measurement of the NM scatter correction factors thus depends on the current integrator being a stable monitor, at least for the period between the free field measurement and the measurement with the fluence measuring equipment in position.

Values for the NM correction factors used at each distance are presented, for the four energies measured, in Table 3 to Table 6. Dead-time corrections were applied to the monitor readings

but in all cases these were small (< 0.9%). Within each table the data are given in the chronological order (from top to bottom of the table) in which they were taken.

At most distances only a single measurement was made at each distance with and without shadow cone. In a few cases, however, repeat measurements without shadow cone were performed, e.g. at 150 cm for 144 keV, and these are included in the tables as a useful indication of the reproducibility of the NM correction factors.

Table 3. Monitor correction factors for measurements at 144 keV

Nominal target to long counter distance	Monitor correction factors		
	Without shadow cone	With shadow cone	Cone identifier
150 cm	1.0058		
150 cm	1.0049	1.0277	NPL #8
200 cm	1.0090	1.0119	NPL #8
250 cm	1.0021	1.0076	NPL #8

All the monitor correction factors are close to unity. For the measurements without shadow cone the differences from unity are all less than 1%. For the measurements with shadow cone the corrections are a little larger, the largest difference from unity being about 2.8%, however, the majority of the correction factors are still within 1% of unity.

Since the NM counts must by multiplied by the correction factors, values greater than unity reflect the fact that the De Pangher or the shadow cone is in some way reducing the number of neutrons reaching the monitor. The geometrical arrangement of the equipment would indicate that the NM is not directly shielded by the fluence measuring equipment, so the explanation for this effect is not immediately apparent.

Monitor counts were recorded by NPL throughout the fluence measurements with the De Pangher long counter. Unfortunately no data was recorded for the free field arrangement so a direct cross check of the PTB monitor correction factors was not possible.

Table 4. Monitor correction factors for measurements at 1.2 MeV

Nominal target to long counter distance	Monitor correction factors		
	Without shadow cone	With shadow cone	Cone identifier
200 cm	1.0023	1.0020	NPL #8
150 cm	1.0037	1.0015	NPL #8
250 cm	0.9992	1.0041	NPL #8
300 cm	0.9990	0.9990	NPL #1
350 cm	0.9997	0.9974	NPL #1
400 cm	0.9993	1.0015	NPL #1
200 cm	1.0033	1.0044	PTB #19
300 cm	1.0000	1.0007	PTB #15

Table 5. Monitor correction factors for measurements at 5.0 MeV

Nominal target to long counter distance	Monitor correction factors		
	Without shadow cone	With shadow cone	Cone identifier
200 cm	09990	0.9902	NPL #8
250 cm	09989	0.9902	NPL #8
300 cm	0.9922	0.9851	NPL #1
300 cm	0.9936		

Table 6. Monitor correction factors for measurements at 14.8 MeV

Nominal target to long counter distance	Monitor correction factors		
	Without shadow cone	With shadow cone	Cone identifier
200 cm	0.9996	0.9956	NPL #8
150 cm	0.9979	0.9954	NPL #8
250 cm	1.0016	0.9963	NPL #8
300 cm	1.0005	0.9921	NPL #1
350 cm	0.9994	0.9906	NPL #1

Monitor corrections were not provided for the PLC. Because of this, and also the fact that the statistics for this device were usually worse than for the NM, the NPL fluence measurements are not reported relative to this monitor. Its (non scatter-corrected) readings were, however, used as an additional check on the consistency of the data collected.

5.2 Target scatter corrections

For the thin targets used to produce the neutron fields used in the present comparison exercise the neutrons emitted at any angle are practically monoenergetic. The energy distribution at a particular angle has a small but finite width, due mainly to energy loss of the charged particle beam in the target material, but with a small additional component due to the finite energy width of the charged particle beam. However, any instrument placed in the neutron field to measure the fluence will detect, in addition to the monoenergetic neutrons, some target scattered neutrons. These are neutrons emitted from the target and then scattered by the material of the target can. For solid targets the majority of the scattering occurs in the target backing. Because the measurements for this comparison were all made at 0^o to the charged particle beam, where the neutron energy is a maximum, and because neutrons lose energy in a scattering process, the target scattered neutrons generally have lower energies than the primary neutrons.

At the PTB a Monte Carlo code, TARGET [(11)], has been written to calculate target scatter spectra, and the results have been validated against time-of-flight measurements. This code was run for the experimental configurations used in the present comparison, and the results

made available to the participants to correct their measurements. The calculated spectra are averaged over the solid angle subtended by the detector, and for this reason results were provided for a range of target to detector distances. Spectra were provided for the direct, i.e. un-scattered, component, the scattered component, and the total. Some typical examples are shown in Figure 6 where only the direct and scattered components are shown for clarity.

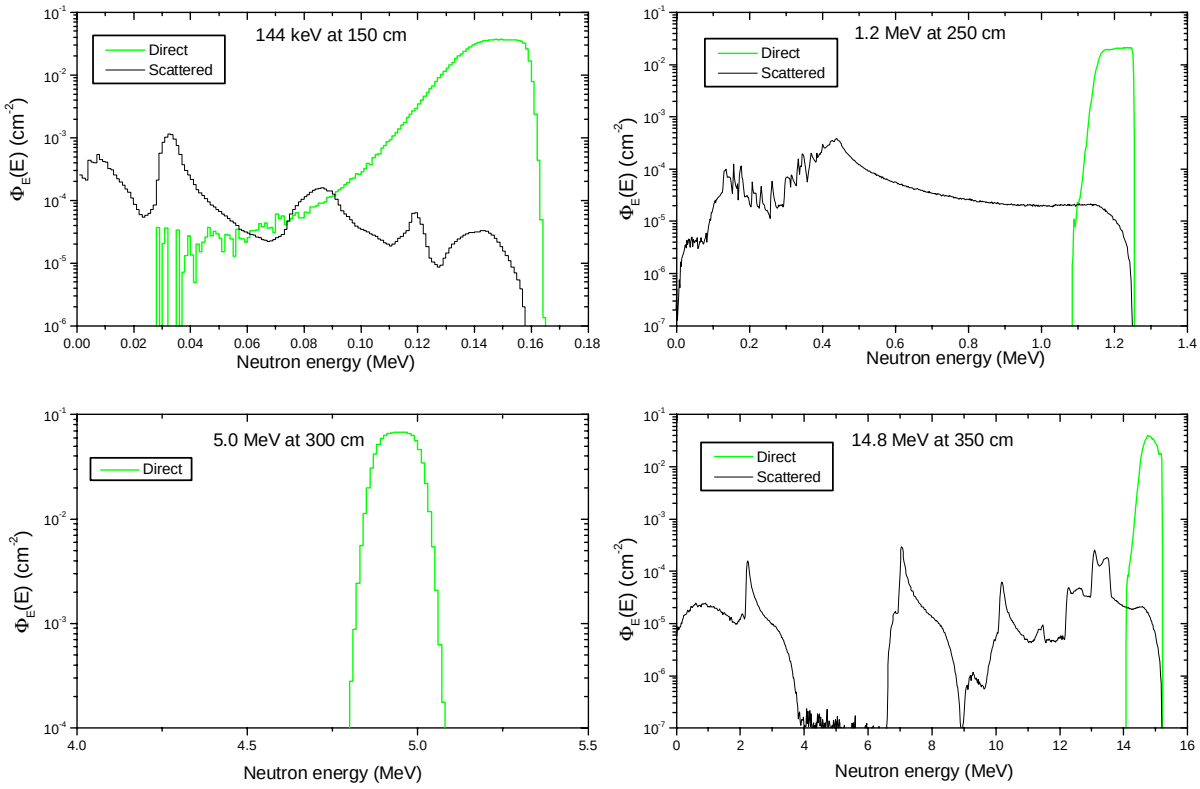

Figure 6. Typical direct and scatter components of the spectra at 144 keV, 1.2 MeV, and 14.8 MeV, and the direct component at 5.0 MeV, as calculated with the TARGET code.

If a long counter is positioned at a distance, l, from a point source the counts, C, can be related to the neutron fluence on the front moderator face of the long counter by:

$$C = \int_0^{E_{max}} \Phi_E(E) \cdot \varepsilon(E) \cdot \frac{l^2}{[l + r(E)]^2} \mathrm{d}E \qquad (1)$$

where:

E_{max} is the maximum neutron energy,
$\Phi_E(E)$ is the differential fluence, $\mathrm{d}\Phi/\mathrm{d}E$, at energy E,
$\varepsilon(E)$ is the long counter efficiency at energy E,
and $r(E)$ is the long counter effective centre at energy E.

The factor $l^2/[l+r(E)]^2$ allows for the fact that when the long counter is used to measure fluence from a point source, it has an effective centre at a distance $r(E)$ from the front face of the moderator. Note that room and air scatter are ignored here. Corrections for these effects are treated separately.

The neutron spectra provided by PTB were given in a number of energy bins, *n* say, rather than as a continuous function. The above expression for the long counter counts thus needs to be re-written as:

$$C = \sum_{i=1}^{n} \Phi_i \cdot \varepsilon_i \cdot \frac{l^2}{[l + r_i]^2} = \sum_{i=1}^{n} \Phi_i \cdot g_i \qquad (2)$$

where:

Φ_i is the total fluence in bin i,
ε_i is the long counter efficiency for the neutrons in bin i,
r_i is the effective centre for neutrons in bin i,
and g_i is a factor equal to $\varepsilon_i \cdot l^2 / [l + r_i]^2$.

The total fluence, Φ_{ti}, in any bin is the sum of the un-scattered, Φ_{ui}, and scattered, Φ_{si}, components, i.e.

$$\Phi_{ti} = \Phi_{ui} + \Phi_{si} \qquad (3)$$

Inserting eq. (3) into eq. (2):

$$C_t = \sum \Phi_{ti} \cdot g_i = \sum \Phi_{ui} \cdot g_i + \sum \Phi_{si} \cdot g_i = C_u + C_s \qquad (4)$$

where:

C_t represents the long counter counts due to the total spectrum from the target,
C_u represents the long counter counts due to the un-scattered spectrum,
and C_s represents the long counter counts due to the target scattered spectrum.

The spectral data provided by PTB were normalised to unity for the direct component, so eq. (4) cannot be used to calculate C_s directly for a particular measurement, however,

$$C_u = C_t - C_s = C_t \left(1 - \frac{C_s}{C_t} \right) = C_t (1 - f_s) \qquad (5)$$

where f_s is the scatter fraction correction to the long counter counts, and because it is derived from the ratio of the scattered to the total counts, these do not need to be known absolutely, i.e. relative values are all that are needed.

A computer program, which used the spectral data as input, was written to calculate the scatter fraction corrections f_s, which were then used to correct the long counter counts to what they would have been in the direct field. A number of other quantities including, the average energy, the average long counter efficiency, and the average effective centre were also calculated.

Table 7 lists the values calculated for f_s at the distances for which spectral information was provided. Since the values only change slightly with distance, corrections for other target to detector distances were derived by interpolation. Values are given for both the old version of

the De Pangher efficiencies and effective centres, and also for the new version. The correction factors are of the order of 2 to 3%, and the differences between the values for the old and the new De Pangher parameters are very small. Because the long counter has an almost constant response as a function of energy over the region of interest, the scatter fraction correction f_s is almost the same as the scattered fluence as a fraction of the total fluence.

Table 7. Calculated scatter fraction corrections f_s used to correct the De Pangher long counter for counts due to target scattered neutrons.

Distance (cm)	Scatter fraction correction f_s					
	144 keV		1.2 MeV		14.8 MeV	
	f_s old	f_s new	f_s old	f_s new	f_s old	f_s new
150	0.0200	0.0202	0.0312	0.0323	0.0198	0.0198
250	0.0198	0.0199	0.0305	0.0319	-	-
350	-		-	-	0.0191	0.0193
400	-		0.0298	0.0315	-	-
450	0.0195	0.0195	-	-	-	-

For the 5 MeV fluences, produced by a deuterium gas target, the calculated spectra provided by the PTB gave the shape of the primary neutron distribution, but included no scatter component so f_s was taken to be zero. Information provided by the PTB about this correction was that: “as a result of the forward peaked angular distribution, target scattered neutrons contribute less than 1% to the total neutron fluence.”

5.3 Long counter data

During the long counter measurements counts were recorded, over a number of cycles, from the CI, the NPL De Pangher, the two PTB monitors, (the NM and the PLC), and from a frequency source running at 10 Hz. This last item provided the time for each cycle which was used when performing dead time corrections. The counts were recorded on a scaler system.

A measurement at a particular energy and target to long counter distance consisted of five cycles for the un-shadowed long counter, and five cycles with an appropriate shadow cone in place. For the 5 MeV measurements five cycles were also recorded with the gas removed from the deuterium gas target cell. Each cycle was for a fixed number of CI pulses, the actual number, in the range 20000 to 100000, depending on the De Pangher count rate relative to the monitor rates. The aim was always to get better than 1% statistical accuracy, and in most cases it was much better than this.

The steps involved in the analysis are outlined below. They were performed using the computer program, FLUCAL, which is normally used at NPL for this task.

1. All the data were analysed statistically to obtain mean values and uncertainties for each block of five cycles.

2. Monitor corrections were applied to the NM counts.

3. Dead time corrections were applied to the De Pangher, the NM, and the PLC. Values used for the dead time per pulse were: 10 μs for the De Pangher, 2.9 μs for the NM, and 5.64 μs for the PLC.

4. Scatter corrections were performed by subtracting the shadow cone measurements from the measurement without shadow cone, the data in both cases being normalised to the CI counts. For the 5 MeV data the gas-out measurement data were also subtracted.

$$M_{CI} = \left[\frac{C_T}{CI_T} - \frac{C_S}{CI_S} \left(- \frac{C_{GO}}{CI_{GO}} \right) \right] \tag{6}$$

where:

C_T, C_S and C_{GO} are the total counts, scattered counts, and where appropriate, the gas-out counts in the De Pangher long counter, and

CI_T, CI_S, and CI_{GO} are the corresponding current integrator counts.

To obtain the value, M_{NM}, for the NM the value of M_{CI} is multiplied by the ratio, CI_T/NM_T, of the CI to the NM counts.

Note the difference between C_T and C_S used above and C_t and C_s used for example in eqs (4) and (5). Upper case subscripts refer to room and air scattering, while lower case subscripts refer to target scattering.

5. The results of step 4 provide the counts due to direct neutrons from the target and these were corrected for target scatter neutrons by multiplying by the appropriate $(1 - f_s)$ factor.

6. The remaining operations involve: correcting for air out-scatter, correcting the results to 1 m, and allowing for the efficiency of the long counter. The fluence, Φ, at 1 m from the target in vacuum was calculated, for both of the direct count per monitor values, M_{CI} and M_{NM}, indicated below simply as M, using eq. (7):

$$\Phi = M \cdot (1 - f_s) \cdot F_{Al} \cdot \frac{(l + \bar{r})^2}{100^2} \cdot \frac{1}{\bar{\varepsilon}} \tag{7}$$

where:

F_{Al} is the air attenuation factor for the target to detector distance, l, given by $F_{Al} = e^{l\Sigma_A}$ where Σ_A is the macroscopic cross section for attenuation in air[5],

l is the target to long counter moderator distance in cm,

$\bar{r}$ is the De Pangher effective centre, in cm, averaged over the direct spectrum,

$\frac{(l + \bar{r})^2}{100^2}$ corrects the measured fluence to the value at 1 m (100 cm), and

$\bar{\varepsilon}$ is the efficiency of the De Pangher averaged over the direct spectrum.

The spectrum averaged parameters $\bar{\varepsilon}$ and $\bar{r}$ were calculated from the spectra provided by the PTB using eqs (8) and (9) below:

$$\bar{\varepsilon} = \sum_{i=1}^{n} \Phi_i \cdot \varepsilon_i / \sum_{i=1}^{n} \Phi_i \tag{8}$$

$$\bar{r} = \sum_{i=1}^{n} \Phi_i \cdot r_i / \sum_{i=1}^{n} \Phi_i \tag{9}$$

the suffix *i* referring to the bin in the energy spectrum.

The values for the efficiency and effective centre obtained by averaging over the spectrum were very little different from those at the mean energy of the direct neutron distribution. The calculations of steps 5 and 6 were performed for both the old and the new long counter data sets, and for both the CI and the NM as monitors.

The distance, *l*, was measured from the front face of the De Pangher moderator to the end of the target can. For the 144 keV, 1.2 MeV, and 14.8 MeV targets 1 mm was added to *l* to give the distance to the neutron producing target layer. For the deuterium gas target 16 mm was added to give the distance to the effective centre of the deuterium gas target.

5.4 Foil data

The activities of the two aluminium foils were measured as soon as they arrived back at NPL. Two separate low-background counters were used. Before being inserted into the counters, the foils were cleaned with ethanol, dried, and then placed on gold-coated VYNS plastic mounts. Both foils were counted for 80 cycles of 2000 seconds after which time sufficient β counts had been recorded to give an acceptably low statistical uncertainty. The background rates of both counters were measured before and after each foil measurement.

A least squares fitting program (MHLIFE) was used to analyse the decay data. The program calculates the saturated β count rate, $N_{\beta(sat)}$ (i.e. that which would be obtained during an infinitely long irradiation at the mean fluence rate). Each β-count cycle is first dead-time corrected, then decay corrected to the end of the irradiation. The decay correction is performed by considering the following integral expression for the counts in each cycle, *C*:

$$C = \int_{t_1}^{t_2} N_\beta \mathrm{e}^{-\lambda t} dt \tag{10}$$

where:

t_1 is the time from the end of the irradiation to the start of the cycle,
t_2 is the time from the end of the irradiation to the end of the cycle,
N_β is the β count rate at the end of the irradiation
λ is the decay constant of the foil activity.

Solving equation (10) yields the following expression:

$$N_\beta = \frac{C\lambda}{e^{-\lambda t_1} - e^{-\lambda t_2}} \tag{11}$$

Another program (NVVARY) analysed the monitor data to calculate the small correction factor for the variation of the fluence rate during the irradiation.

The total neutron fluence, Φ, is related to the saturated foil activity, $N_{0,}$ by:

$$N_0 = [\Phi / T]\sigma(E_n)(mf_a N_A / A) \tag{12}$$

where:

T is the irradiation time,
$\sigma(E_n)$ is the activation cross section at neutron energy E_n,
m is the mass of the foil,
f_a is the isotopic abundance,
N_A is Avogadro's number,
A is the atomic weight.

The value of $\sigma(E_n)$ at the mean neutron energy is obtained by interpolating between tabulated values, and the mean neutron energy was calculated from the target scattered spectrum supplied by PTB. The saturated activity is related to the β count rate at saturation, $N_{\beta(sat)}$ by:

$$N_{\beta(sat)} = N_0 \varepsilon'_\beta F_T F_a(d) \tag{13}$$

where:

ε'_β is the effective β-efficiency (allowing for the γ-ray sensitivity of the β-detector by means of the K-correction),
F_T is the fluence rate variation correction factor,
$F_a(d)$ is the self shielding factor for a foil, thickness d.

For the foil thicknesses used the self shielding is negligible, hence $F_a(d) = 1$, and the effect of the front foil shielding the back is also negligible.

Finally $N_{\beta(sat)}$ is related to the β count rate, N_β, at the end of the irradiation by:

$$N_\beta = N_{\beta(sat)}\left(1 - e^{-\lambda T}\right) \tag{14}$$

where:

λ is the decay constant.

Combining the above equations gives the expression for the fluence, Φ:

$$\Phi = \frac{N_\beta \cdot T}{\sigma(E_n)(mf_a N_A / A)\varepsilon'_\beta F_T F_a(d)} \cdot \frac{1}{(1 - e^{-\lambda T})} \tag{15}$$

Values for N_β for each β counting cycle are obtained from eq. (11).

An 'effective distance' of each foil from the target layer was calculated allowing for the target backing thickness of 0.5 mm, the foil thickness of 0.26 mm, and the radii of the foil and beam spot. The beam spot was assumed to be 1 cm in diameter. Corrections were applied for air out-scatter and for target scattered neutrons (see Section 5.2). Finally the fluence measured by each foil was corrected to a distance of 1 m from the target.

The mean of the two foils was calculated and divided by the CI counts, or the in-scatter and dead-time corrected NM count, recorded during the irradiation.

6 Results

6.1 144 keV measurements

Table 8 gives the results for the fluence per CI, and per NM, at the nominal neutron energy of 144 keV, and also lists all the data required to derive these values from the De Pangher long counter counts, *M*, corresponding to detection of the direct neutron fluence. The corrections for room and air in-scatter, made when deriving *M* from the total counts, varied from 2.4% at 150 cm to 4.2% at 250 cm. Data are presented for the measurements at each of the three target to long counter distances, and also for both the old and the new De Pangher parameters.

Table 8. Results for measurements at 144 keV at three distances

Parameters	Results for individual distances		
Nominal distance	150 cm	200 cm	250 cm
Shadow cone no.	NPL #8	NPL #8	NPL #8
M_{CI}	1.433	0.8096	0.5115
NM/CI	0.5107	0.5106	0.5107
M_{NM}	2.806	1.586	1.002
f_s old	0.0200	0.0199	0.0198
f_s new	0.0202	0.0201	0.0199
F_{Al}	1.029	1.039	1.048
l (cm)	150.0	199.6	250.0
$\bar{r}$ old (cm)	2.04	2.04	2.04
$\bar{r}$ new (cm)	2.08	2.08	2.09
$\bar{\varepsilon}$ old (cm^2)	3.281	3.280	3.280
$\bar{\varepsilon}$ new (cm^2)	3.193	3.194	3.194
Φ/CI old (cm^{-2})	1.018	1.021	1.018
Φ/CI new (cm^{-2})	1.046	1.049	1.046
Φ/NM old (cm^{-2})	1.994	2.000	1.993
Φ/NM new (cm^{-2})	2.049	2.055	2.048

New-old % diff.	2.8 %	2.7 %	2.7 %

From analysis of the TARGET code spectra provided by the PTB staff[10] the mean energies of the direct spectra, integrated over the front face of the De Pangher, varied from 144.1 keV at 150 cm to 144.8 keV at 250 cm. These changes are simply a result of the variation of the neutron energy with angle, and the variation of the solid angle subtended by the long counter as the distance changes. Long counter efficiency and effective centres were calculated separately for each distance, however, the variations are extremely small as shown in Table 8.

In Figure 7 the consistency of the results as a function of target to long counter distance are illustrated, and also the differences between the results obtained with the old and the new De Pangher parameters. Data are only presented for the fluence relative to the CI as a monitor. Because the ratio of the NM pulses to the CI pulses was practically constant for the three measurements, a plot of the data relative to the NM is identical in appearance except for a different normalisation. (Although, for some energies, the ratio NM/CI varied over the day, for the measurements with the NPL De Pangher long counter at 144 keV, 1.2 MeV, and 14.8 MeV, the ratio was constant within the uncertainties over the period of the measurements.)

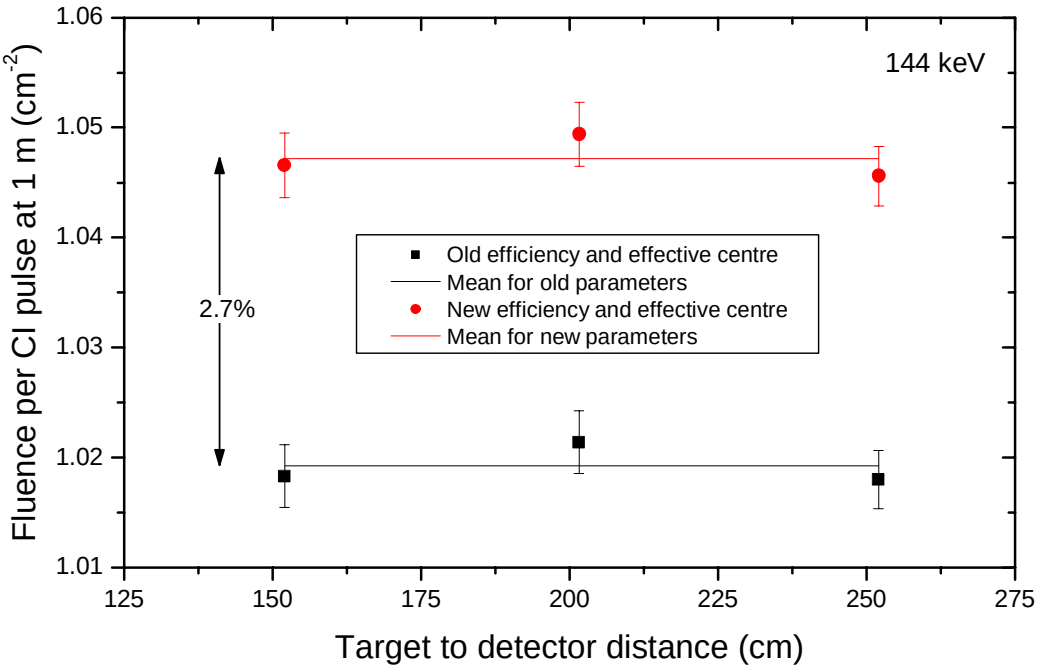

Figure 7. Results for fluence per CI pulse at 144 keV

The error bars for the fluence values in Figure 7, and in all subsequent figures in this section, are a reasonable but not exact estimate of those uncertainties which are **not** common to measurements at different distances, i.e. the uncorrelated components. The uncertainties which are effectively 100% correlated, e.g., the De Pangher efficiency, were excluded. There are also some uncertainty components which are correlated for measurements at different distances, but are not 100% correlated (the precise degree of correlation being difficult to quantify). These are discussed in more detail in the section on uncertainties, but these are also excluded from the error bars shown in the plots. Their contribution would not be large, however, their

exclusion means that the error bars represent a lower limit for the true uncorrelated uncertainties. The components which were actually included in the error bars were those due to: statistics, uncertainty in the dead time correction (taken to be 10% of the correction), and a component for the uncertainty in the distance *l*.

In can be seen from Figure 7 that there was very good agreement between measurements at different distances, but that the fluences derived using the old and the new De Pangher long counter parameters differed by about 2.7%. These results will be discussed in more detail in Section 8, "Summary, discussion, and conclusions".

6.2 1.2 MeV measurements

Table 9 lists, in two parts (a) and (b), the results for the measurements at 1.2 MeV. These were performed at six different target to long counter distances, and at two of the distances measurements were performed with shadow cones belonging to the PTB in addition to those made with the NPL shadow cones. Corrections for room and air in-scatter ranged from 2.7% at 150 cm to 9.7% at 400 cm.

The mean energies of the direct spectra, integrated over the front face of the De Pangher long counter, varied from 1.199 MeV at 150 cm to 1.204 MeV at 400 cm.

Table 9(a). Results for measurements at 1.2 MeV at four distances

Parameters	Results for individual distances			
Nominal distance	150 cm	200 cm	250 cm	300 cm
Shadow cone no.	NPL #8	NPL #8	NPL #8	NPL #1
M_{CI}	4.521	2.581	1.643	1.138
NM/CI	1.620	1.620	1.620	1.621
M_{NM}	2.790	1.593	1.014	0.7021
f_s old	0.0312	0.0308	0.0304	0.0302
f_s new	0.0323	0.0321	0.0319	0.0318
F_{Al}	1.015	1.020	1.025	1.030
l (cm)	150.2	199.6	250.2	299.7
$\bar{r}$ old (cm)	4.19	4.20	4.20	4.20
$\bar{r}$ new (cm)	0.61	0.56	0.51	0.49
$\bar{\varepsilon}$ old (cm^2)	3.685	3.685	3.686	3.686
$\bar{\varepsilon}$ new (cm^2)	3.460	3.460	3.460	3.460
Φ/CI old (cm^{-2})	2.876	2.876	2.868	2.848
Φ/CI new (cm^{-2})	2.918	2.951	2.963	2.956
Φ/NM old (cm^{-2})	1.774	1.775	1.770	1.758
Φ/NM new (cm^{-2})	1.801	1.821	1.829	1.824
New-old % diff.	1.5 %	2.6 %	3.3 %	3.8 %

Table 9(b). Results for measurements at 1.2 MeV at four distances

Parameters	Results for individual distances			
Nominal distance	350 cm	400 cm	200 cm	300 cm
Shadow cone no.	NPL #1	NPL #1	PTB #19	PTB #15
M_{CI}	0.8337	0.6356	2.570	1.138
NM/CI	1.621	1.620	1.621	1.620
M_{NM}	0.5144	0.3922	1.586	0.7024
f_s old	0.0300	0.0298	0.0308	0.0302
f_s new	0.0316	0.0315	0.0321	0.0318
F_{Al}	1.035	1.040	1.020	1.030
l (cm)	350.0	400.0	199.6	299.7
$\bar{r}$ old (cm)	4.20	4.20	4.20	4.20
$\bar{r}$ new (cm)	0.48	0.47	0.56	0.49
$\bar{\varepsilon}$ old (cm^2)	3.686	3.686	3.685	3.686
$\bar{\varepsilon}$ new (cm^2)	3.459	3.459	3.460	3.460
Φ/CI old (cm^{-2})	2.850	2.845	2.863	2.849
Φ/CI new (cm^{-2})	2.968	2.969	2.937	2.957
Φ/NM old (cm^{-2})	1.758	1.755	1.767	1.758
Φ/NM new (cm^{-2})	1.831	1.832	1.813	1.825
New-old % diff.	4.2 %	4.4 %	2.6 %	3.8 %

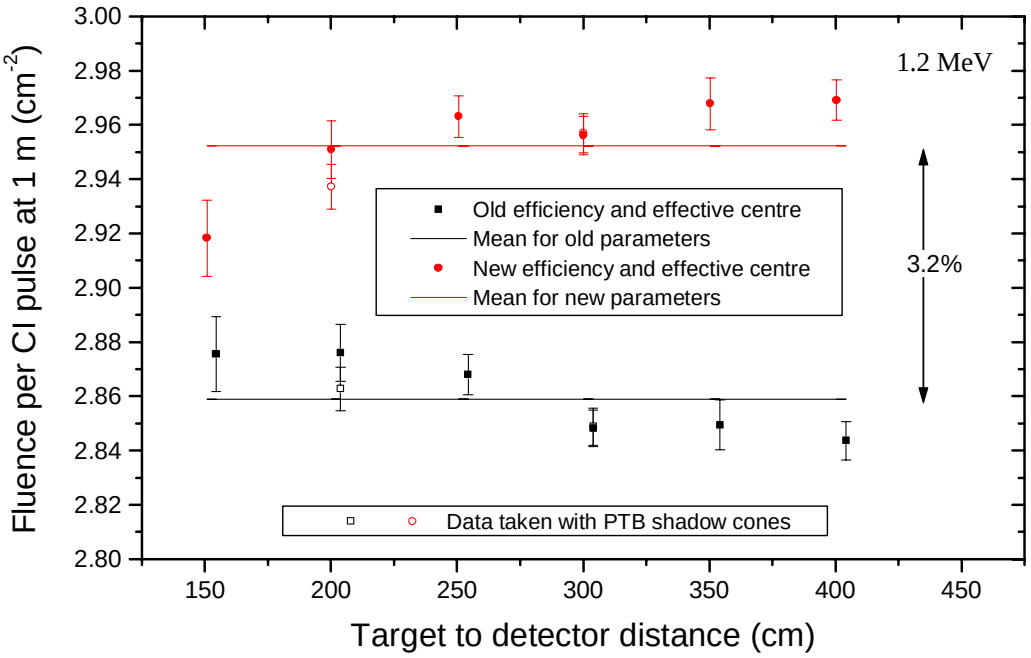

Figure 8. Results for fluence per CI pulse at 1.2 MeV

Figure 8 presents the results as a function of distance for both the old and the new De Pangher long counter parameters. As for the results at 144 keV, the data at 1.2 MeV are only presented in terms of the fluence per CI pulse. The figure for the fluence per NM would look almost identical. There is reasonable agreement between results at different distances, although not as good as at 144 keV. The difference between the results using the old and the new De Pangher parameters is a little larger than at 144 keV.

At 200 cm and 300 cm measurements were performed with both NPL and PTB shadow cones. Mounting arrangements for the two sets of cones were rather different, however, there was excellent agreement between the fluence results obtained using the different cones. This gives confidence in the operation of the shadow cone technique, and also reassurance that the rather ad hoc mounting arrangements for the NPL shadow cone were quite adequate. A full discussion of the results is left until after the discussion of the uncertainties.

6.3 5.0 MeV measurements

One additional step was required for the measurements at 5 MeV compared to the other three energies. Because a gas target was used a 'gas-out' measurement was performed, and this was done after the 'total' and shadow cone measurements at each distance. The values for *M/CI* and *M/NM* shown in Table 10 have been corrected by subtracting the 'gas-out' counts. These amounted to about 1% of the 'total' counts. These were smaller than the in-scatter corrections measured using the shadow cones which ranged from 2.1% at 200 cm to 3.4% at 300 cm.

Table 10. Results for measurements at 5 MeV at three distances

Parameters	Results for individual distances		
Nominal distance	200 cm	250 cm	300 cm
Shadow cone no.	NPL #8	NPL #8	NPL #1

M_{CI}	11.065	7.768	5.465
NM/CI	5.256	5.669	5.666
M_{NM}	2.105	1.370	0.9644
f_s old	0.0	0.0	0.0
f_s new	0.0	0.0	0.0
F_{Al}	1.014	1.017	1.020
l (cm)	199.8	250.3	300.0
$\bar{r}$ old (cm)	9.29	9.29	9.29
$\bar{r}$ new (cm)	6.88	6.87	6.85
$\bar{\varepsilon}$ old (cm^2)	3.408	3.408	3.408
$\bar{\varepsilon}$ new (cm^2)	3.335	3.334	3.334
Φ/CI old (cm^{-2})	14.38	15.62	15.65
Φ/CI new (cm^{-2})	14.37	15.67	15.75
Φ/NM old (cm^{-2})	2.737	2.755	2.762
Φ/NM new (cm^{-2})	2.733	2.764	2.779
New-old % diff.	-0.1 %	0.3 %	0.6 %

The mean energies of the direct spectra, integrated over the front face of the De Pangher long counter, varied from 4.938 MeV at 200 cm to 4.941 MeV at 300 cm.

The results are presented graphically in Figure 9 where values are shown for both the fluence per CI pulse and the fluence per NM pulse. For a gas target which is emptied for a 'gas-out' measurement between fluence measurements (or between a fluence measurement and an instrument measurement during a normal calibration), the CI is not an appropriate monitor because it is almost impossible to refill the gas cell to exactly the same gas pressure, and the neutron production per unit charge depends directly on the gas pressure. This is demonstrated clearly in Figure 9 where it can be seen that there is only rather poor consistency between fluence values per CI pulse at different distances, whereas the agreement for the fluence per NM pulse at the three distances is excellent.

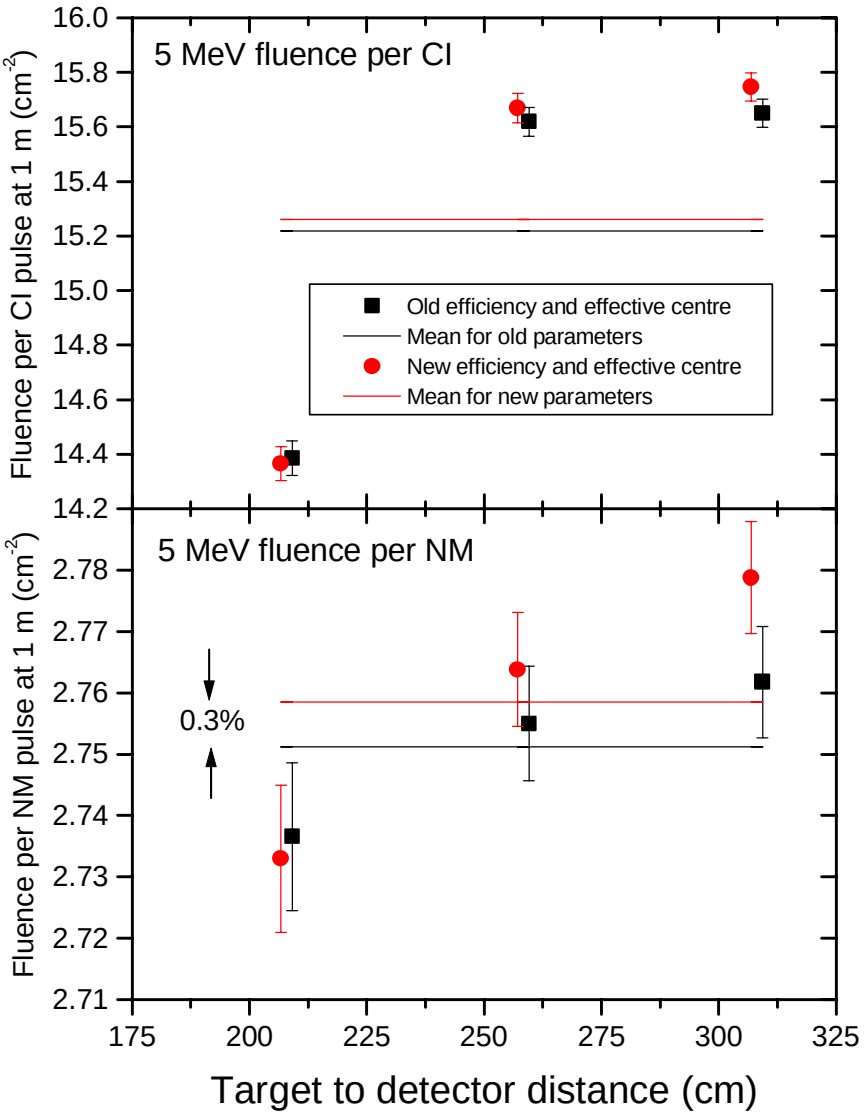

Figure 9. Results for fluence per CI pulse and fluence per NM pulse at 1.2 MeV

At 5 MeV not only is there reasonable agreement between the fluence values per NM pulse at different distances, there is also excellent agreement when using either set of De Pangher long counter parameters. This is despite the fact that the parameters themselves differ significantly.

6.4 14.8 MeV measurements

6.4.1 De Pangher long counter measurements

Although long counters are not routinely used at NPL to measure fluences in the region of 14.8 MeV, measurements were performed at the PTB with the NPL De Pangher long counter, and the results are shown in Table 11. Measurements were performed at five different distances, and the mean energies, integrated over the front face of the De Pangher varied from 14.845 MeV at 150 cm to 14.847 MeV at 350 cm.

Table 11. Results for measurements at 14.8 MeV with the long counter at five distances

Parameters	Results for individual distances				
Nominal distance	150 cm	200 cm	250 cm	300 cm	350 cm

Shadow cone no.	NPL #8	NPL #8	NPL #8	NPL #1	NPL #1
M_{CI}	17.733	10.015	6.583	4.620	3.403
NM/CI	8.604	8.596	8.608	8.618	8.625
M_{NM}	2.061	1.165	0.7647	0.5361	0.3946
f_s old	0.0198	0.0196	0.0195	0.0193	0.0191
f_s new	0.0198	0.0197	0.0196	0.0194	0.0193
F_{Al}	1.012	1.016	1.020	1.024	1.028
l (cm)	150.3	202.4	250.7	300.7	350.9
$\bar{r}$ old (cm)	14.99	14.99	14.99	14.99	14.99
$\bar{r}$ new (cm)	9.54	9.54	9.54	9.54	9.54
$\bar{\varepsilon}$ old (cm^2)	2.515	2.515	2.515	2.514	2.514
$\bar{\varepsilon}$ new (cm^2)	2.284	2.284	2.284	2.284	2.284
Φ/CI old (cm^{-2})	19.11	18.75	18.49	18.40	18.28
Φ/CI new (cm^{-2})	19.68	19.63	19.53	19.56	19.53
Φ/NM old (cm^{-2})	2.222	2.182	2.148	2.135	2.120
Φ/NM new (cm^{-2})	2.287	2.283	2.268	2.270	2.264
New-old % diff.	3.0 %	4.6 %	5.6 %	6.3 %	6.8 %

In Figure 10 the results are presented graphically for the fluence per CI pulse. The values at the different distances are quite consistent when analysed using the new De Pangher parameters, but are not for the old parameters. In addition there is a significant difference of about 5.1% between the mean of the results obtained using the new parameters and the mean of those using the old parameters. Also shown in Figure 10 is the result from the aluminium foil measurement. The agreement with the De Pangher result, using the new parameters, is within about 1%.

If the data is presented per NM count the shape of the plot for the long counter results is almost identical to that per CI pulse, except for the normalisation. However, the agreement between the aluminium foil results and those for the long counter, when using the new parameters, is even better, the difference being only about 0.1%. This is due to variations in the NM/NM ratio over the day and is discussed further in Section 8.

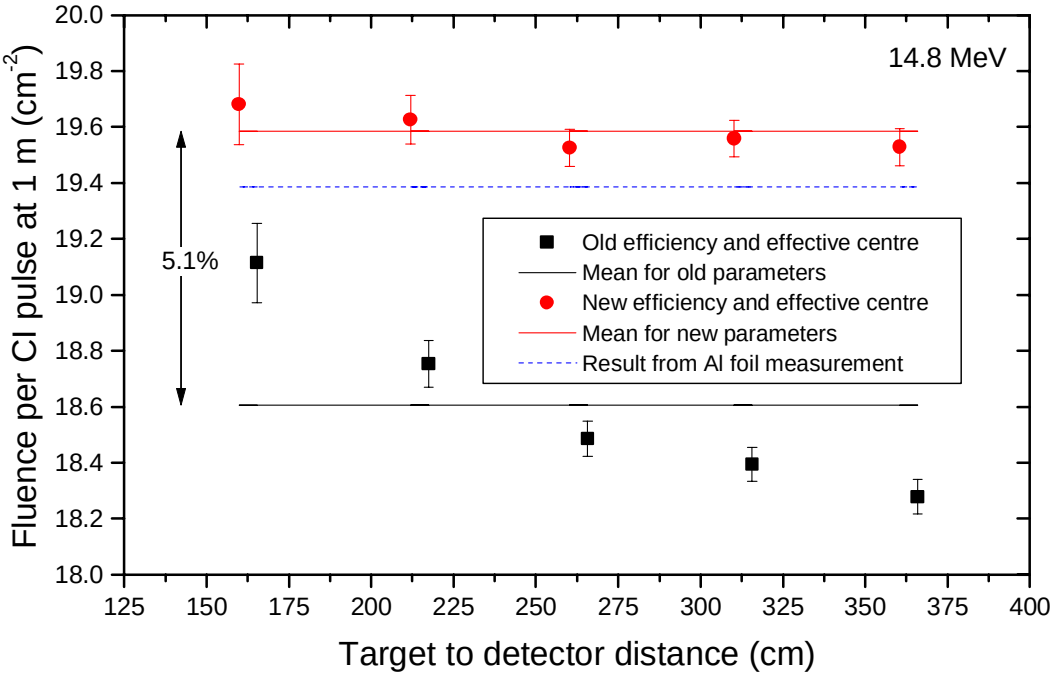

Figure 10. Results for fluence per CI pulse at 14.8 MeV

Table 12. Results for measurements with the aluminium foils at 14.8 MeV

Input parameters	Foils	
	Al28	Al30
Mass (mg)	395.560	395.190
ε_β'	0.7381	0.7381
$N_\beta(s^{-1})$	90.673	90.389
$\lambda\ (s^{-1})$ [12]	1.2866×10^{-5}	
f_a	1.00	
A [13]	26.9815	
T (s)	12800	
CI total counts	4 487 741	
NM total counts	37 810 534	
NM in-scattering correction factor	1.0012	
NM dead time factor	1.0086	
Target scatter factor, f_s	0.0101	
F_T	1.0005	
$F_a(d)$	1.0	
Effective distance (cm)	9.114	9.138
Air attenuation factor (0.85 % m^{-1})	1.0008	1.0008
Mean neutron energy, E_n	14.845 MeV	
$\sigma(E_n)$ [14]	111.09 mb	
Φ [@1 m in vacuum] (cm^{-2})	8.684×10^7	8.711×10^7
Mean Φ [@1 m in vacuum] (cm^{-2})	8.698×10^7	
Φ/CI (cm^{-2})	19.381	
Φ/NM (cm^{-2})	2.278	

6.4.2 Aluminium foil measurements

Table 12 gives the results for the fluence per CI pulse, and per NM count, from the measurements with the two aluminium foils, which were labelled Al28 and Al30, and also lists all the data used to derive these results.

As can be seen, there is excellent agreement between the results from the two foils.

7 Calculation of the uncertainties.

The treatment of the uncertainties in this report follows the recommendations of the *Guide to the Expression of Uncertainty in Measurement, GUM*, [15]. All uncertainties are estimates of the standard uncertainty, i.e. they are estimates at the 1σ, 67% confidence, level.

7.1 Uncertainties in the De Pangher long counter measurements

The fluence is derived from the measured De Pangher data using eq. (7). This has been re-written below with the air attenuation term $F_{Al}\ (=\mathrm{e}^{l\Sigma})$ written out explicitly, the subscripts dropped from f_s and Σ_A, and the 'bar', indicating a mean value, dropped from the variables r and ε for simplicity in the subsequent expressions.

$$\Phi = M \cdot (1-f) \cdot \mathrm{e}^{l\Sigma} \cdot \frac{(l+r)^2}{100^2} \cdot \frac{1}{\varepsilon} \tag{16}$$

If the reasonable assumption is made that in the above equation the effect of the uncertainty in l on $\mathrm{e}^{l\Sigma}$ is negligible compared to the uncertainty in Σ, then all the input parameters can be treated as if they occur only once in eq. (16), and the combined variance, $u_c^2(\Phi)$, for a fluence measurement at a single target to long counter distance is given [15], in terms of the standard uncertainties in the individual quantities, *u(M), u(f),* etc., by:

$$\begin{aligned} u_c^2(\Phi) = &\left(\frac{\partial \Phi}{\partial M}\right)^2 \cdot u^2(M) + \left(\frac{\partial \Phi}{\partial f}\right)^2 \cdot u^2(f) + \left(\frac{\partial \Phi}{\partial \Sigma}\right)^2 \cdot u^2(\Sigma) \\ &+ \left(\frac{\partial \Phi}{\partial l}\right)^2 \cdot u^2(l) + \left(\frac{\partial \Phi}{\partial r}\right)^2 \cdot u^2(r) + \left(\frac{\partial \Phi}{\partial \varepsilon}\right)^2 \cdot u^2(\varepsilon) \end{aligned} \tag{17}$$

where:

$$\left(\frac{\partial \Phi}{\partial M}\right) = \frac{\Phi}{M} \tag{18}$$

$$\left(\frac{\partial \Phi}{\partial f}\right) = \frac{-\Phi}{(1-f)} \tag{19}$$

$$\left(\frac{\partial \Phi}{\partial \Sigma}\right) = \Phi \cdot l = \Phi \cdot \frac{(l\Sigma)}{\Sigma} \tag{20}$$

$$\left(\frac{\partial \Phi}{\partial l}\right) = 2 \cdot \frac{\Phi}{(l+r)} \tag{21}$$

$$\left(\frac{\partial \Phi}{\partial r}\right) = 2 \cdot \frac{\Phi}{(l+r)} \tag{22}$$

$$\left(\frac{\partial \Phi}{\partial \varepsilon}\right) = \frac{\Phi}{\varepsilon} \tag{23}$$

Since all the above differentials involve the fluence, Φ, eq. (17) can be written in terms of the fractional variance for the fluence as:

$$\begin{aligned}\left(\frac{u_c(\Phi)}{\Phi}\right)^2 = &\left(\frac{u(M)}{M}\right)^2 + \left(\frac{f}{(1-f)} \cdot \frac{u(f)}{f}\right)^2 + \left(l\Sigma \cdot \frac{u(\Sigma)}{\Sigma}\right)^2 \\ &+ \left(2 \cdot \frac{u(l)}{(l+r)}\right)^2 + \left(2 \cdot \frac{u(r)}{(l+r)}\right)^2 + \left(\frac{u(\varepsilon)}{\varepsilon}\right)^2\end{aligned} \tag{24}$$

In cases where the uncertainty in the input quantity is usually expressed as a percentage, the variables in eq. (24) have deliberately been arranged in terms of the fractional uncertainty in the quantity.

It is obvious from the above that the combined uncertainty is not a simple quadratic sum of the uncertainties in the input parameters. This is because of the forms of the expressions for the sensitivity coefficients. For example the sensitivity coefficient for the uncertainty in the effective centre, *r*, is 2/(*l*+*r*), i.e. it depends on the distance *l*, and the effect of the uncertainty in *r* decreases as *l* increases.

The uncertainty in *M* in made up of several components, see eq. (6) for the formula for calculating *M*. Statistical uncertainties apply to the long counter counts and they must be included. An uncertainty component is also included for the dead time correction, and a further uncertainty is included to allow for the fact that the shadow cone measurement does not give a perfect estimate of the scattered neutron component. Finally a component is included for the stability of the long counter as a function of time – see section 3.2.

Statistical uncertainties in the total and scatter counts were derived from the spread of the results during the five cycles of measurement and also from assuming Poisson statistics. The value used was the larger of these two. Statistical uncertainties represent a very small fraction of the final uncertainty in the fluence so this pessimistic approach does not affect the final value. The dead time correction uncertainty was then added in quadrature with the statistical uncertainty, for both the total and scatter counts, and the uncertainty in the in-scatter corrected counts derived from the expression for the uncertainty in the difference of two numbers. An additional component of 5% of the in-scatter correction was then added in quadrature to allow for uncertainty in the shadow cone technique, and finally the contribution for the long counter stability was added. Where the long counter counts were 'per NM count', the statistical uncertainty in the NM count was added in quadrature when determining the final fluence uncertainty.

Eq. (24) is the appropriate formula for calculating the uncertainty for a measurement at a single target to long counter distance. However, the derivation of the best result from a set of measurements at a small number of different distances, and in particular the calculation of the uncertainty for the combined results, presents additional problems. These arise because the results of the measurements at different distances are not independent, but are correlated in a complex way.

Of the six uncertainty components shown in eq. (24) one, the uncertainty component for the distance l, is effectively independent for each measurement so that the contribution to the uncertainty at different distances is completely uncorrelated. Two contributions to the final uncertainty, those due to the uncertainty in the quantities f and ε, are not dependent on the distance l (except for a completely negligible dependence resulting from the small changes in the spectrum with distance) and are hence 100% correlated between measurements at different distances. For the other three components there is an element of correlation, but this is less than 100%. For Σ and r the reason for this is fairly obvious. Although the same value is used for Σ and r at each distance, the expressions for the uncertainty contributions in eq. (24) involve the distance l as well as the quantity Σ or r. For long counter counts, M, correlations arise from using a common dead time per pulse in the dead time correction, from the uncertainty components allowing for the fact that the shadow cone technique is not perfect, and from the uncertainty component for the long term stability of the long counter.

When a routine fluence determination is made at NPL, a measurement is only made at a single target to long counter distance. The opposite extreme is a measurement of the effective centre distance, r, when data are taken at 30 or more distances, over as wide a range of distances as possible, (about 1 m to 5 m). The data are then analysed, using least squares techniques, for r as well as for the fluence. The present measurements represent a situation somewhere between these two extremes. A rigorously correct mathematical approach to deriving the 'best value' for the fluence from measurements at a small number of distances, and equally importantly determining the uncertainty for this best value is presently being investigated at NPL. The methodology of the uncertainty analysis is complex, and the mathematical technique is not yet finalised. In the meantime, for the analysis of the present data, a simple pragmatic approach has been taken.

The usual approach to determining the best value from the few available results would be a weighted mean, with the weights reflecting the appropriate uncertainties, i.e. those which are

uncorrelated. In the present case the effects of the uncertainties in f and ε are common (100% correlated) at all distances, and so can be excluded from the weights. The uncertainty due to l is independent for each measurement and should therefore be included. For each of the parameters M, Σ, and r, the uncertainties at the various distances are correlated to some degree. Ideally only the uncorrelated part should be included in the weights. However, the fluence results at different distances, for a particular set of long counter parameters (new or old), are usually very consistent. The weighted mean would thus be relatively insensitive to the weights. The approach adopted for deriving the best value was thus to use the combined uncertainty calculated from those in M,Σ, l, and r, when deriving the weights; those in f and ε being excluded. At all four energies all the data, i.e. all the distances, were included in the weighted mean.

It should be noted that the partial uncertainty contribution derived from combining those in M,Σ, l, and r, does not vary greatly over the range of distances for which measurements were made. One reason for this is that some contributions to the uncertainty increase with distance, e.g. that due to the uncertainty in Σ, and that due to the shadow cone correction uncertainty, while other contributions decrease with distance, e.g. that due to the uncertainty in r. In fact there is a minimum in the value of this partial uncertainty contribution, the distance at which this minimum occurs depending on the particular uncertainties chosen for the input parameter. This can be seen as representing the optimum distance at which to make a measurement.

Because the uncertainties used for calculating the weights are not truly independent, the conventional formula for determining the uncertainty of a weighted mean should not be used. The uncertainty actually quoted is the minimum value from those at the various distances. This was not always the optimum position as described above because the range of measurements did not include the optimum distance. For this set of measurements, the smallest uncertainty was that for the largest distance, because of the large contribution from the uncertainty in r.

The consistency, within the uncertainties, of the results at different distances, provides strong evidence that the values used for the input parameters and their uncertainties are reasonable. The actual values are discussed in section 8.

7.2 Uncertainties in the foil measurements

The value for the fluence from the foil measurements is obtained from eq. (15) which only involves multiplication or division by all the input parameters except λ. The combined uncertainty in the fluence from all the components except λ can thus be derived from a simple quadratic sum of the percentage uncertainties in the input parameters.

To investigate the sensitivity of the uncertainty in Φ on the uncertainty in λ the expression for N_β in terms of the measured β counts C (eq. (11)) must be included in eq. (15). For the purposes of an uncertainty analysis, the decay correction of eq. (11) can be simplified by:

$$N_\beta = \frac{C\lambda}{\mathrm{e}^{-\lambda t_1} - \mathrm{e}^{-\lambda t_2}} \approx \frac{C \cdot \mathrm{e}^{\lambda t_m}}{\Delta t} \tag{25}$$

where:

t_m is the time from the end of the irradiation to the midpoint of the β counting period,

and Δt is the counting period i.e. $(t_2 - t_1)$.

Use of this simplified expression for N_β in eq. (15) enables the sensitivity coefficient for the uncertainty component due to the half-life to be evaluated. The overall dependence of Φ on λ is given by:

$$\Phi \propto \frac{e^{\lambda t_m}}{(1-e^{-\lambda T})} \tag{26}$$

and the sensitivity coefficient is thus:

$$\left(\frac{\partial \Phi}{\partial \lambda}\right) = \Phi\left[t_m - \frac{T \cdot e^{\lambda T}}{(1-e^{-\lambda T})}\right] \tag{27}$$

Using eq. (27) the contribution to the uncertainty in Φ due to the uncertainty in the decay constant λ can be calculated and added in quadrature to the sum of the other uncertainties.

The negative sign in the sensitivity coefficient reflects the fact that the dependence of Φ on the decay constant λ is different for the two terms which make up eq. (26). The term $e^{\lambda t_m}$ corrects for decay of the activity between the irradiation and the counting of the activity, whereas the term $(1-e^{-\lambda T})$ corrects for incomplete saturation. The dependence of Φ on λ is opposite for the two terms. Interestingly, for a particular combination of t_m and T the sensitivity coefficient actually becomes zero.

8 Summary, discussion, and conclusions

8.1 Summary of final results

The NPL results for this key comparison exercise are given in Table 13, together with the estimated standard uncertainties. Fluence values are quoted both 'per CI count' and 'per NM count' at all energies except 5 MeV where the CI was not an appropriate monitor. The results at 144 keV, 1.2 MeV, and 5.0 MeV are from the De Pangher long counter measurements, and represent a weighted mean of measurements at several distances. The 14.8 MeV results are from the aluminium foil measurements made at 9 cm from the target. All results are, however, quoted at 1 m from the target in vacuum.

Table 13. NPL key comparison results for the fluence at 1 m from the target in vacuum.

Energy	Fluence per CI count (cm^{-2})	Fluence per NM count (cm^{-2})
144 keV	1.047 ± 0.024	2.051 ± 0.045
1.2 MeV	2.958 ± 0.071	1.826 ± 0.044
5.0 MeV	-	2.762 ± 0.064
14.8 MeV	19.38 ± 0.21	2.278 ± 0.030

For the De Pangher measurements two results were available at each energy corresponding to the old and the new long counter efficiency and effective centre values. Only one result can be quoted for a key comparison, and the decision was taken to quote the value corresponding to the new parameters for all three energies. For 5 MeV the choice is immaterial since the old and new results agree, but at 144 keV and 1.2 MeV the two results differ. The decision to use the new parameters was based mainly on the fact that improved calculational information was available when determining the new values of the parameters[7]. This should result in more accurate values. However, the new calculated effective centre values have yet to be fully validated against experiments, and it is well to bear in mind that the NPL long counters have been used in international comparison exercises in the past, using the old parameter values, and excellent agreement has been achieved with other participants[1]. All the above issues were taken into consideration when determining values for the uncertainty components for the efficiencies and effective centres at the different energies.

Table 14 lists the component uncertainties which, when combined according to eq. (24), give the standard uncertainty in the fluences deduced from the De Pangher measurements. All the values quoted are assumed to be estimates of standard uncertainties and have normal probability distributions.

Table 14. Component uncertainties for the De Pangher long counter measurements at 144 keV, 1.2 MeV and 5.0 MeV

Input parameters	Neutron energy		
	144 keV	1.2 MeV	5.0 MeV
Statistics & dead time	0.2%	0.2%	0.3%
Scatter correction	0.2%	0.5%	0.2%
De Pangher stability	0.4%	0.4%	0.4%
M*	0.5%	0.7%	0.5%
f_s	10%	10%	10%
Σ_A	10%	10%	10%
l	0.2 cm	0.3 cm	0.2 cm
r	0.5 cm	2.0 cm	1.0 cm
ε	2.0%	2.0%	2.0%
Combined uncertainty CI results	2.1%	2.4%	2.2%
NM statistics	0.2%	0.2%	0.2%
NM stability[16]	0.4%	0.4%	0.8%
Combined uncertainty NM results	2.2%	2.4%	2.3%

* The uncertainty for M is the quadratic sum of the three components above

The statistical uncertainties in the NM counts quoted in Table 14 derive from the data taken by NPL. The uncertainties in the stability were obtained from data provided by PTB staff for the variation of the NM/CI ratio as observed from repeat ‘free field’ measurements.

The uncertainties in Table 13 and Table 14 correspond to the measurement at the target to long counter distance which gave the lowest uncertainty. For 144 keV this was 250 cm, for 1.2 MeV it was 400 cm, and for 5.0 MeV it was 300 cm.

Table 15 shows the uncertainty components for the activation foil measurements. All components have essentially an infinite number of degrees of freedom.

Table 15. Component uncertainties for the aluminium foil measurements at 14.8 MeV

Symbol	Source of uncertainty	Value (%)	Probability distribution	Divisor	u_i (%)
	Counting statistics	0.1	normal	1	0.1
F_T	Flux variations	0.005	normal	1	0.005
$\varepsilon_{ß}$	ß-counting efficiency	0.2	normal	1	0.2
K	K-correction	0.2	normal	1	0.2
$\sigma(E)$	Activation cross section	0.5	normal	1	0.5
E_n	Mean neutron energy (20 keV)	0.38	rectangular	$\sqrt{3}$	0.22
m	Foil mass	0.1	rectangular	$\sqrt{3}$	0.06
λ	Decay constant	0.01	normal	1	0.01
	Dead time correction	0.2	rectangular	$\sqrt{3}$	0.12
	Target – foil distance (0.7 mm)	1.5	rectangular	$\sqrt{3}$	0.89
f_s	Target scatter factor	0.05	normal	1	0.05
$u(\varphi)$	Combined uncertainty CI results	---	normal	---	1.1
	NM statistics	0.02	normal	1	0.02
	NM stability[16]	0.6	normal	1	0.6
$u(\varphi)$	Combined uncertainty NM results	---	normal	---	1.3

8.2 Discussion of the measurements

At the present time an investigation of the best values for the long counter efficiencies and effective centres, and also, most importantly, the uncertainties on these parameters, is being undertaken at NPL following an earlier careful re-estimation of efficiency values based mainly on detailed MCNP calculations[7]. No final decision has yet been reached on the best values, and information from the present comparison exercise will be used as input to this process. For this reason the uncertainties quoted here for these two parameters depend a little on the consistency of the results derived using the new and the old values for the parameters. The uncertainties used over recent years at NPL for the old effective centre and efficiency values were 0.5 cm and 1.5 % respectively. Comparison of the new and old values for these parameters indicates that these estimates may have been a little optimistic.

8.2.1 144 keV measurements

Measurements were performed at three distances, 150 cm, 200 cm, and 250 cm. For the new values of the De Pangher long counter parameters the agreement between the three results is excellent – see Figure 7. The results analysed with the old parameters also agree very well with each other, but there is a difference of 2.7% between the two sets of results. Both the new and the old effective centre values are almost identical, so the difference derives solely from the difference in the efficiency values. The uncertainties assigned to the effective centre and efficiency values were 0.5 cm and 2% respectively.

8.2.2 1.2 MeV measurements

The data at 1.2 MeV provide useful input to the problem of determining the most appropriate long counter parameters. Measurements were performed at six distances, ranging from 150 cm to 400 cm, and the agreement between these data are not quite as good as might be expected considering the uncertainties – see Figure 8. The results for both the new and old parameters vary with the measurement distance used, the variations being in opposite directions. This would appear to indicate that the effective centres used were not quite correct, and that the correct value probably lies somewhere between the two.

As was the case for the 144 keV measurements, the mean values for the two sets of results differ, in this case by 3.2%. In contrast to the case for the 144 keV data, where the new and old effective centre values were very similar, the situation at 1.2 MeV is that both the effective centre and the efficiency differ significantly between the new and old estimates. The efficiency values differ by just over 6% on average, while the effective centres differ by a factor of seven or more! In view of these differences, it is perhaps surprising that the fluences derived form the new and old parameters differ by only 3.2%. The reason for this is that there is an element of cancellation. The term involving r and ε which occurs in the expression for the fluence is, $(l + r)^2/\varepsilon$, and the effects of the differences in the efficiency and effective centre act in opposite directions. Values for this quantity are presented in Table 16, together with the differences between the new and the old estimates.

Table 16. Values of the term $(l + r)^2/\varepsilon$, used in calculating the fluence, at the various measurement distances

		Measurement distance in cm					
		150	200	250	300	350	400
$(l + r)^2/\varepsilon$	new	6572	11579	18168	26048	35508	46361
	old	6469	11270	17559	25056	34036	44323
Difference		1.6%	2.7%	3.4%	3.8%	4.1%	4.4%

One surprising feature of the new parameters is the small value, of the order of 0.5 cm, for the effective centre. As the energy increases the neutrons would be expected to penetrate to increasing depths within the long counter moderator, and for the effective centre to thus increase continuously with increasing energy. There is an extent to which this does occur in the calculational results, however, there is also some very marked structure in the plot of effective centre against energy. This is illustrated in Figure 11 which shows the variation of the MCNP calculated effective centre values near 1.2 MeV, and also the shape of the 1.2 MeV fluence distribution as derived from the TARGET code [10]. There is a very noticeable dip in

the effective centre values just above 1.2 MeV. No explanation has yet been found for this effect, it does not tie-in with structures in the carbon total cross section, and it can be seen from the large number of calculated points in this region that it is not simply due to a single (erroneous) calculated value. The effective centre used was obtained by integrating the spectral distribution with the effective centre variation, and the value derived in this way is quite sensitive to the exact energy of the fluence distribution.

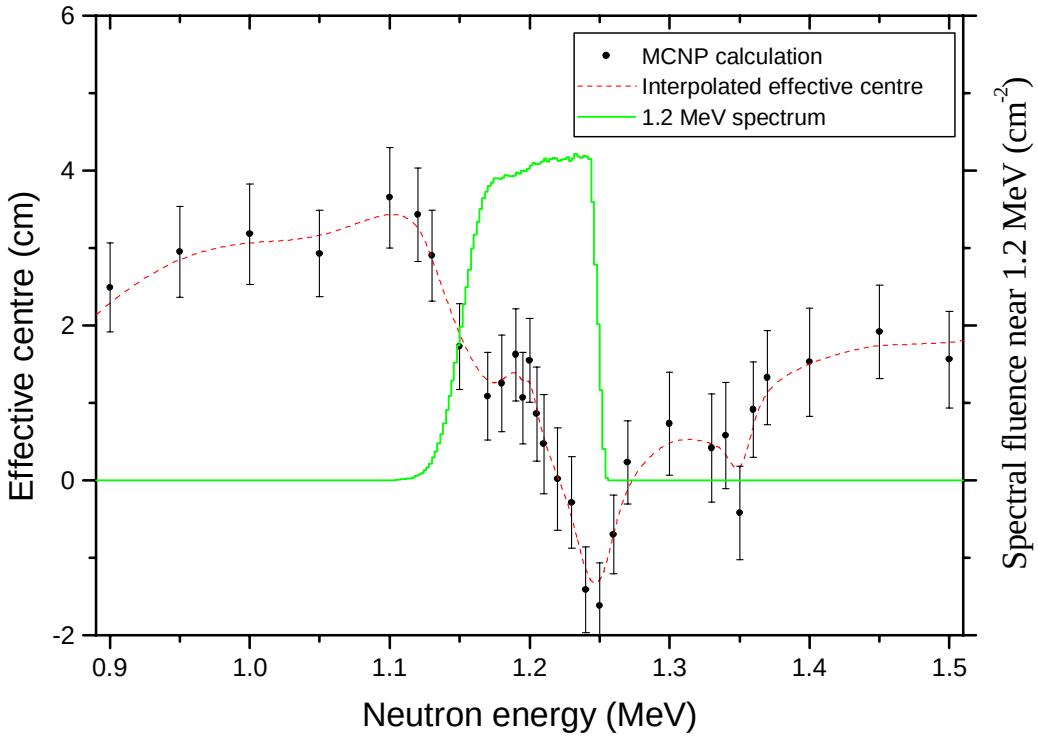

Figure 11. The variation of the new calculated effective centre values near 1.2 MeV

In view of the difference between the new and the old effective centres, and the unexplained structure shown in Figure 11, an uncertainty of 2 cm was assigned to the effective centre at 1.2 MeV. The uncertainty in the efficiency was estimated as 2%

8.2.3 5.0 MeV measurements

At 5 MeV the fluence values calculated with both the new and the old long counter parameters agree with each other. When presented relative to the NM, the results at the three distances where measurements were made also agree very well. There is slightly better agreement as a function of distance for the results with the old parameters, see Figure 9, but this is not significant considering the uncertainties.

Although the new and the old parameters give essentially the same result, this is not because the parameters themselves are the same. The new efficiency value is about 2.2% lower than the old, and the new effective centre is about 26% (2.4 cm) lower than the old. However, the term $(l + r)^2/\varepsilon$ which occurs in the calculation of the fluence is almost identical for the two sets of parameters, and this explains the excellent agreement. Although this agreement helps give confidence in the present results, it will unfortunately be impossible to extract any information from the present exercise on which set of parameters is the most accurate.

In view of the differences between the old and new parameters, the uncertainties assigned to the effective centre and efficiency values were 1.0 cm and 2% respectively.

No target scatter corrections were applied at this energy since no target scatter spectra were available. According to information from the PTB the target scatter fluence should be less than 1% of the total fluence. Because the NPL measurements were performed with a long counter, which has a near constant response over the energy range for both direct and scattered neutrons, any target scatter neutrons which were present will be included in the quoted fluence. No allowance has been made for this in the uncertainty budget.

8.2.4 14.8 MeV measurements

The use of aluminium foils as transfer devices for measuring fluences in the 14 MeV region is well established. For the present exercise two foils were used, and the agreement between the two results is excellent. The difference is only about 0.3% which is quite satisfactory agreement in the light of the size of the uncertainty components which are not correlated between the two results. These are, the statistics (0.1%), the β counting efficiency (0.2%), and some element of the distance uncertainty, i.e. that arising from any gap between the foils. The final combined uncertainty in the fluence is quite small, at just over 1%, indicating that for fluence measurements in this region foil activation provides comparable uncertainty to primary standard techniques.

Comparison of the foil results and those from the De Pangher long counter show remarkable agreement provided the new parameters are used in analysing the long counter data. Figure 10 shows the values per CI pulse where the difference is less than 1%. Assuming an effective centre uncertainty of 2 cm, the mean result for the long counter data per CI pulse is 19.56 cm^{-2}, c.f. the slightly lower value of 19.38 cm^{-2} from the foil data. The good agreement for the new parameters, and the variation of the results for analysis with the old parameter values as a function of distance, provides evidence that the new parameters are more appropriate than the old in this energy region.

If the results per NM count are compared, rather than per CI pulse, the agreement between the foil result of 2.278 cm^{-2} and the long counter result, which is 2.271 cm^{-2} for the new parameters, is even better. The difference is then only about 0.3%. Note that the foil result is now slightly higher than the long counter result. The reason for the difference between the results per CI pulse and per NM count stems from the fact that the yield from the target, per CI pulse, increased continuously over the day of the measurement, a fact which was noted by the PTB staff from analysis of the free-field measurements[16]. The two measurements were separated in time by several hours, the foil measurements being performed near the beginning of the run, and the De Pangher measurements near the end.

8.3 Conclusions

The first part of the present key comparison exercise, i.e. the acquisition and analysis of the data, has been completed successfully. However, the true value of the exercise will not become evident until the next stage, i.e. the comparison of the results presented by the various participants.

Some useful information has already emerged from the work to date. It has been shown that standards instruments such as long counters can successfully be taken to other laboratories and measurements performed. The use of activation foils as a transfer device has been shown to be feasible, despite the relatively short half-life of about 15 hours for the ^{24}Na activity produced in the aluminium foils. Finally the agreement between the aluminium foil results and those derived from the De Pangher long counter measurements with the new values for the efficiency and the effective centre give some direct support for the use of the new parameters, in the 14 MeV region at least.

Acknowledgements

We would like to thank the scientific staff at the PTB, in particular Drs Horst Klein and Sigmund Guldbakke, for their generous help in all matters connected with the comparison, and Dr Dietrich Schlegel for providing the results of the TARGET calculations. Thanks also go to the operators of the PTB Van de Graaff for their very efficient operation of the accelerator, and Nicky Horwood at NPL for help with the organisation.

References

1. R.S. Caswell and V.E. Lewis, *Neutron measurement intercomparisons sponsored by CCEMRI, Section III (Neutron Measurements)*, Radiat. Prot. Dosim. 44, 105-110, 1992.

2. International Organization for Standardization, *Reference neutron radiations – Part 1: Characteristics and Methods of production*, International Standard ISO 8529-1 2001.

3. M.H. McTaggart, *A study of the Neutron Long Counter*, AWRE Report NR/A-1/59, 1959.

4. J. De Pangher and L.L. Nichols, *A Precision Long Counter for Measuring Fast Neutron Flux Density*, Pacific Northwest Laboratory Report BNWL-260, 1966.

5. J.B. Hunt, *The Calibration and Use of Long Counters for the accurate measurement of Neutron Flux Density*, NPL Report RS(EXT)5, April 1976.

6. J.F. Briesmeister, editor, *MCNP – A General Monte Carlo N-Particle Transport Code*, Oak Ridge National Laboratory, LANL Manual LA-12625-M Version 4B, Los Alamos, 1997.

7. H. Tagziria and D.J. Thomas, *Re-calibration and Monte Carlo modelling of the NPL long counters*, NPL Report CIRM 19, September 1998.

8. J.E. Perry, *Neutron Flux Measurements*, Chapter IV.B in Fast Neutron Physics, Part I, editors J.B. Marion and J.L. Flower, Interscience Publishers, Inc., 1960.

9. D.J. Thomas and V.E. Lewis, *Standardisation of neutron fields produced by the $^{3}H(d,n)^{4}He$ reaction*, Nucl. Instrum. and Meths. 179, 397-404, 1981.

10. D. Schlegel, PTB, *private communication*, 2001.

11. D. Schlegel, *Target User's Manual, PTB Laboratory Report PTB-6.41-1998-1*, April 1998.

12. IAEA TECDOC-619; *X-ray & Gamma-ray Standards for Detector Calibration*, (IAEA, Vienna 1991)

13. P. Möller, J. R. Nix, W. D. Myers, and W. J. Swiatecki, *Nuclear Ground-State Masses and Deformations*, Atomic Data and Nucl. Data Tables 59, 185-381 (1995)

14. M. Wagner, H. Vonach, A. Pavlik, et al., Physics Data 13-5 (Fachinformationszentrum Karlsruhe, 1990).

15. *Guide to the Expression of Uncertainty in Measurement*, prepared by a joint BIPM, IEC, IFCC, ISO, IUPAC, IUPAP, and OIML working group and published by ISO.

16. S. Guldbakke, PTB, *private communication*, 2002.